In presenting the dissertation as a partial fulfillment of the requirements for an advanced degree from the Georgia Institute of Technology, I agree that the Library of the Institute shall make it available for inspection and circulation in accordance with its regulations governing materials of this type. I agree that permission to copy from, or to publish from, this dissertation may be granted by the professor under whose direction it was written, or, in his absence, by the Dean of the Graduate Division when such copying or publication is solely for scholarly purposes and does not involve potential financial gain. It is understood that any copying from, or publication of, this dissertation which involves potential financial gain will not be allowed without written permission.

7/25/68

THE COMPOSITION OF COMPLEX METAL HYDRIDES IN ETHER SOLVENTS

A THESIS

Presented to

The Faculty of the Graduate Division

by

Frank R. Dobbs

In Partial Fulfillment

of the Requirements for the Degree

Doctor of Philosophy in the

School of Chemistry

Georgia Institute of Technology

December, 1972

THE COMPOSITION OF COMPLEX METAL HYDRIDES IN ETHER SOLVENTS

Approved:

Chairman

Date Approved by Chairman: October 16, 1972

To My Wife, Mary Ann

ACKNOWLEDGEMENTS

The author wishes to thank his advisors, Dr. E. C. Ashby, and Dr. Harry P. Hopkins of Georgia State University for their guidance throughout the course of this work. Dr. Ashby suggested this problem, and his interest and enthusiasm were instrumental in its successful completion. A special thanks is due Dr. Hopkins for his efforts in the design and fabrication of a high vacuum conductance cell system, and in the successful development of the mathematical treatment of the data. The author also wishes to express his gratitude to Dr. E. Grovenstein, Jr. for his useful suggestions during the reading of the first draft of this thesis.

The author has held an instructorship during the academic year at Georgia Tech and a PRF assistantship during the summer months for which he is grateful. A special acknowledgement is due Dr. W. M. Spicer for the opportunity to teach chemistry at the Georgia Institute of Technology and Georgia State University.

The author would like to acknowledge the encouragement of his parents and family toward the completion of this endeavor. The author wishes to thank his wife, Mary Ann, and his daughter for their patience, encouragement, and help during these studies.

TABLE OF CONTENTS

LIST OF TABLES

LIST OF TABLES (Continued)

LIST OF TABLES (Continued)

LIST OF ILLUSTRATIONS

SUMMARY

The complex metal hydrides behave as weak electrolytes in tetrahydrofuran. The equivalent conductances for lithium aluminum hydride, sodium aluminum hydride, tetrabutylammonium aluminum hydride and lithium borohydride in THF are consistent with the presence of free ions and ion pairs in dilute solution, and the formation of triple ions at the higher concentrations. In the region where free ions and ion pairs are encountered, the limiting equivalent conductances (Λ_o) and the ion pair dissociation constants (K_a) are evaluated by the Fuoss method. Utilizing a sphere in continuum model, the center-to-center distances between the ions in the ion pair calculated from the experimental K_a values indicate that the ion pairs of Bu_4NAlH_4 and $LiBH_4$ are in intimate contact, whereas the $LiAlH_4$ and $NaAlH_4$ species are solvent separated ion pairs. Furthermore, the thermodynamic parameters suggest that a substantial fraction of the $NaAlH_4$ ion pairs are in intimate contact at 25°C, while the $LiAlH_4$ ion pairs are predominantly solvent separated. The Λ_o values obtained for these hydrides support these results. In the region where ion pairs and triple ions are encountered, the triple ion dissociation constants (K_t) have been evaluated from the data using the Fuoss method. Combining the K_a and K_t values, the fraction of each species present at any concentration below 0.1 M has been calculated. When these values are used to calculate a predicted i-value, a good agreement is found between the observed ebullioscopic i-values and those predicted from the conductance results. NMR studies indicate the formation of a 4:1 THF solvate with

$LiAlH_4$, $LiClO_4$ and LiI, and the formation of a 2:1 THF solvate with $LiBH_4$. Bu_4NAlH_4 shows no interaction with THF in similar studies. The appearance of bands near 420 cm^{-1} in the infrared, which are attributed to the vibration of the lithium ion in a solvent cage, are found for $LiAlH_4$, $LiClO_4$, LiI and LiBr, but well defined bands are absent for $LiBH_4$ in THF. The alkoxy derivatives of $LiAlH_4$ and $LiBH_4$ in THF can also be interpreted in terms of ion pairs, triple ions and larger aggregates. Except for $LiAl(OCH_3)H_3$, the methoxy compounds show extensive association in THF as the concentration is increased. The other alkoxy derivatives exist primarily as ion pairs, since the i-value does not exceed 1.2 over the concentration range studied. NMR and infrared studies suggest the formation of a lithium ion-carbonyl complex with acetone in diethyl ether and THF. From these results, a reasonable model for the mechanism of $LiAlH_4$ reduction of ketones involving initial complexation of the carbonyl group by lithium ion followed by subsequent rearrangement and hydride transfer is proposed.

CHAPTER I

INTRODUCTION

Background

Since the discovery of lithium aluminum hydride and lithium borohydride by Schlesinger[1] and coworkers, thousands of reports[2] concerning the use of these compounds as reducing agents in organic synthesis have appeared in the literature. The availability of these ether-soluble reducing reagents has provided the organic chemist with a means of performing selective reductions on organic substrates, which prior to this time, were not possible. Few details, however, are presently available on the mechanism of these reductions. The lack of precise information concerning the nature of the solute species in ethereal solvents has been the major obstacle in providing an exact description of the mechanism of complex metal hydride reduction of organic substrates. Thus, in spite of the fact that reductions of ketones and other organic functional compounds by $LiAlH_4$ represents one of the most fundamental reactions in all of organic chemistry, it has not been possible to describe the mechanism of these reactions in any detail. Consequently, it would appear that information concerning the nature of the solute species present in ether solutions

of complex metal hydrides, such as $LiAlH_4$, is crucial before a precise description of the mechanism of reduction can be deduced.

Concuctance data on solutions of $LiAlH_4$ are indeed meager due to the extremely reactive nature of the hydride with trace amounts of water. The only available data is limited to concentrations above 0.05 M. In diethyl ether the conductance of $LiAlH_4$ is reported by Paddock[3] to be 4.43×10^{-5} ohm^{-1} cm^{-1} for a 1 M solution, which is approximately the same value reported for ethylmagnesium bromide under similar conditions. Evans and coworkers[4] obtained values of a similar order of magnitude for the conductance of $LiAlH_4$ in diethyl ether over the entire concentration range 0.04 m to 0.32 m. The data of Jarder[5] in the same concentration range follows an identical trend but the actual conductance values reported are an order of magnitude larger than those reported by Evans. In tetrahydrofuran (THF), Alpatova[6] reported the conductance of $LiAlH_4$ in the concentration range 0.1 M to 0.5 M to be similar to the results obtained in diethyl ether except that the values were increased by a hundredfold.

In addition to $LiAlH_4$, conductance data on ethereal solutions of $NaAlH_4$ and $LiBH_4$ are meager. The conductance of a 3 M solution of $NaAlH_4$ in THF at 40 C is reported to be 2×10^{-2} ohm^{-1} cm^{-1} by Alpatova.[6] The conductance[7] of a 0.5 M solution of $LiBH_4$ in diethyl ether is reported to

be less than 1 x 10^{-6} ohm^{-1} cm^{-1} and the conductance of a 0.3 M solution of $LiBH_4$ in THF is reported to be 7.7 x 10^{-5} ohm^{-1} cm^{-1} at 25°C. Conductance data and molecular association data are not available for ethereal solutions of the alkoxy derivatives of $LiAlH_4$ and $LiBH_4$.

The crystal structures[8,9] and infrared spectra[10] for $LiAlH_4$ and $LiBH_4$ have been determined, establishing the tetrahedral symmetry of the AlH_4^- and the BH_4^- ions. In solution the presence of ionic species (I) or covalent species (II) has not been definitely established even though both types have been proposed as existing in solution.

$Li^+AlH_4^-$

I

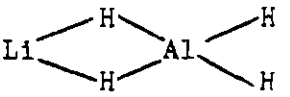

II

Previous molecular weight and conductance studies on these hydrides have suggested that some form of association of the solute occurs in solution. Wiberg and Graf[11] performed crude molecular weight experiments on $LiAlH_4$ in diethyl ether and found that the solute was extensively associated. Extensive association of $LiBH_4$ was also observed in diethyl ether by Nöth.[7] It has been proposed that the observed association is due to the formation of hydrogen bridge species (III).

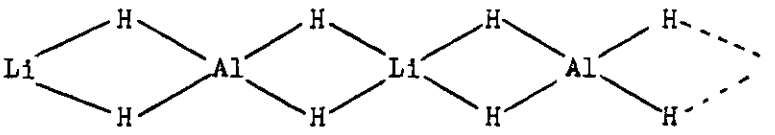

III

Four Raman and two infrared bands have been observed for $LiAlH_4$ in diethyl ether by Lippincott.[12] The coincidence of the infrared bands with the Raman bands is consistent for the tetrahedral model of the AlH_4^- ion in solution. These results have been substantiated by D'Or and Fuger.[13] A similar result is reached by Haraguchi and Fujiwara,[14] who observed that the aluminum —27 signal for $LiAlH_4$ in diethyl ether is similar to the chemical shift and line width of other aluminum compounds known to possess tetrahedral symmetry.

A distorted tetrahedral symmetry for the AlH_4^- ion has been suggested by several other investigators.[15,16] There is a shift to lower wave numbers for the Al-H stretching band in the infrared spectra of diethyl ether (1740 cm^{-1}) and THF solutions (1698 cm^{-1}) of $LiAlH_4$ compared to that found in the solid (1798 cm^{-1}). A shift is also found in a solution of $LiAlH_4$ in benzene-THF where the ratio of $LiAlH_4$:THF is 1:3 (1724 cm^{-1}) and 1:8(1674 cm^{-1}). The frequency of the Al-H stretching band, however, is independent of concentration for diethyl ether solutions of $LiAlH_4$ even

though the association increases with increasing concentration.

Purpose

The limited association data supports the concept of hydrogen bridged species (III), whereas the conductance and spectral data suggests that the tetrahedral symmetry of the AlH_4^- ion is retained in solution, i.e., ionic species (I). Before this question can be resolved and kinetic data can be unambiguously interpreted, the exact nature of the solute species present in solution must be determined.

To provide this information, extensive conductance (0.5 M to 1×10^{-7} M) and ebullioscopic (0.5 m to 0.05 m) measurements were obtained on lithium aluminum hydride, sodium aluminum hydride, tetrabutylammonium aluminum hydride, lithium borohydride and several alkoxy derivatives of $LiAlH_4$ and $LiBH_4$. From these data and the data from NMR and infrared studies, an exact description of the solute species present in THF solution has been developed. A reasonable model for the reduction of ketones with complex metal hydrides is proposed in terms of these solute species. The effect of these solute species on the stereoselectivity of these reductions is also examined.

CHAPTER II

EXPERIMENTAL

Materials

Lithium aluminum hydride, sodium aluminum hydride and lithium borohydride were obtained from Alfa Inorganics (98%+ pure), and were used without further purification.

Fisher reagent grade tetrahydrofuran (THF) and diethyl ether were distilled over $LiAlH_4$ in a nitrogen atmosphere.

Fisher reagent grade methanol was distilled from magnesium turnings.

Fisher reagent grade tert-butyl alcohol was distilled from sodium.

Fisher reagent grade benzophenone was distilled twice under vacuum.

Lithium bromide, lithium iodide, and lithium perchlorate were obtained from Alfa Inorganics and were used without any further purification.

Tetrabutylammonium bromide was obtained from Eastman, recrystallized twice from THF and dried on a high vacuum line.

Apparatus and Procedure

Conductance Measurements

The conductances of solutions were measured on a Beckman Model RC-18A conductivity bridge. The reported accuracy is ± 0.05% of the decade resistance reading over the range 500-50,000 ohms. A Sargent (Model S-

82055) constant temperature water bath was employed for regulating temperatures of the solution between 0°C and 25°C, using a thermometer read to the nearest 0.01°C which was calibrated against a NBS resistance thermometer. For temperatures below 0°C, an isopropyl alcohol — carbon dioxide slush bath containing appropriate amounts of water was employed with an iron-constantine thermocouple ($\pm$1.0°) to determine the temperature of the bath.

A high vacuum system was designed to obtain reproducible conductance data below 3×10^{-3} M, where it is essential to remove all traces of oxygen and water if hydrolysis is to be avoided. Two types of conductance cells were employed and are shown in Figure 1. Cell I consisted of a one liter flask with: A, a vacuum magnetic stirrer (Scientific Glass No. JS-3085 24/40) inserted through a 24/40 joint; B, a Beckman conductivity cell (Model Cel-A001-Y87) sealed to the bottom of the flask; C, a side arm for the storage and introduction of hydride samples. This flask was attached to a standard high vacuum system and was flamed until the pressure was below 5×10^{-5} torr. Sealed ampoules containing the hydrides were then moved from the side arm into the flask and broken by means of a teflon coated magnetic stirring bar. Known amounts of THF were transferred to the conductance cell from a storage flask on the vacuum rack through a buret with a vacuum stopcock. The storage flask contained a saturated solution of $LiAlH_4$ in THF. With this arrangement, reproducible data were obtained down to 5×10^{-5} molar hydride.

In order to obtain reproducible data below 5×10^{-5} M, it was necessary to employ Cell II. This cell consisted of storage flask (D), a condenser (E), an oblong conductance flask (F) with calibration marks

on the side for volume determination, a side arm (G) for sample bulb storage and introduction, a 29/40 joint to insert a Beckman conductivity cell (H) into the flask, and a teflon high vacuum stopcock (J). This cell was attached to a high vacuum system, and the THF was introduced as described previously. After the removal of the cell from the vacuum system with stopcock (J) closed, a sample of hydride was introduced into the cell and allowed to react with any water present. When the conductance was constant, this solution was poured into storage flask (D). Then THF was distilled back into the cell to wash out any remaining hydride. When the conductance of the distilled THF was less than 0.40×10^{-6} mhos (the conductance of the pure THF is 0.40×10^{-6} mhos), a new sample bulb was broken. To obtain lower concentrations, an appropriate amount of this solution was poured into storage flask (D) and pure THF distilled back into the cell to effect the desired dilution. With this procedure conductance data were obtained on each hydride down to 2×10^{-7} M. Even with this procedure it was difficult to determine accurately the conductance of $LiAlH_4$ solutions below 1×10^{-6} M.

For concentrations above 0.01 M, a normal conductance cell purged with nitrogen was employed. A Beckman conductivity cell (Model Cel-A001-Y87) or conductivity cell (Model 3401, Yellow Springs Instrument Co.) was inserted into an oblong flask of the type shown in Figure 1, and allowed to cool under a nitrogen purge. A known volume of solvent (about 100 ml) was transferred to the flask through a teflon stopcock via a syringe. Aliquots of approximately 1.0 M hydride were then transferred to the flask via syringe to obtain the desired concentrations. Effective mixing of the

solution was accomplished by means of a magnetic stirring bar.

For the dilute concentration range, samples of hydride were prepared in sealed ampoules. A 10-500 mg sample of the approximately 1.0 molar stock solution, which was stored in a recirculating dry box[19,20] at all times, was transferred to an ampoule sealed to a 10/18 joint by means of a syringe. The exact weight of the sample of hydride was determined by difference. After the second weighing of the ampoule and 10/18 joint, the lower portion of the ampoule was immersed in liquid nitrogen, and the ampoule bulb was sealed and removed from the stopcock with a torch.

The cell constant of both cells I and II were determined from the measured conductivity of a 0.01 demal potassium chloride solution.[17,32] The constants are 0.00958 cm^{-1} $\pm$ 0.0001 for both cells. For a check on the entire apparatus, the conductances of aqueous acetic acid solutions were measured between 10^{-5} M and 10^{-4} M and found to agree within 0.1% of the published data.[18] For the higher concentrations of hydrides, a cell having a constant of 1.123 cm^{-1} $\pm$ 0.002 was employed.

Preparation of Solutions of the Complex Metal Hydrides

Concentrated solutions of $LiAlH_4$, $NaAlH_4$ and $LiBH_4$ in THF and of $LiAlH_4$ and $LiBH_4$ in diethyl ether were prepared from commercially available hydrides and freshly distilled solvent by stirring at 25°C for three days. The solutions were filtered in a recirculating dry box[19,20] to remove the excess solids to give clear, colorless solutions. The elemental ratios ($\pm$1.0%) for the THF solutions of $LiAlH_4$, $NaAlH_4$ and $LiBH_4$ were respectively: Li/Al/H = 1.0/1.0/4.0, 1.0/1.0/4.0, Li/H = 1.0/4.0. The elemental ratios ($\pm$ 1.0%) for the diethyl ether solutions of $LiAlH_4$ and

$LiBH_4$ were respectively: Li/Al/H = 1.0/1.0/4.0, Li/H = 1.0/4.0.

All the alkoxy derivatives were prepared according to the procedure of Brown[22] and coworkers. The preparation of $LiAl(OCH_3)H_3$ in THF illustrates the preparative scheme. To a 250 ml flask that was flamed and allowed to cool under nitrogen was added 150.0 millimole of $LiAlH_4$ (150.0 ml of 1.0 M $LiAlH_4$) via calibrated syringe. The solution was cooled in an ice bath, and stirring was accomplished by means of a magnetic stirring bar. Through a two way stopcock, 150 millimoles of methanol (4.80 g, 6.0 ml) was added dropwise to the flask via a calibrated syringe. The evolution of gas ceased quickly upon addition of the alcohol. The concentration of the solution was then determined.

In general, the alkoxy derivatives were prepared in THF by the addition of precise stoichiometric amounts of alcohol or ketone to a known quantity of hydride at 0°C. The reaction is essentially quantitative, since no unreacted alcohol or ketone was detected in the distillate from these hydride solutions by either IR or GLC. All of the alkoxy derivatives gave colorless solutions in THF without the formation of a precipitate except $LiAl(OCH_3)_3H$, which underwent disproportionation slowly according to the following equation:

$$2\ LiAl(OCH_3)_3H \rightleftharpoons LiAl(OCH_3)_2H_2 + LiAl(OCH_3)_4$$

A solution of $LiAl(OCH_3)_3H$ (1.0 M) remained clear for approximately 24 hours at 25°C. Then a white solid precipitated having low hydridic activity (H/Al = 0.29), while the solution still retained a high degree of hydridic activity (H/Al = 1.88). Typical analyses for the alkoxy

derivatives of $LiAlH_4$ are presented in Table 1.

The preparation of the alkoxy derivatives of $LiBH_4$ in THF required longer reaction times. $LiB(O\text{-}tBu)H_3$ and $LiB(O\text{-}tBu)_3H$ were prepared at reflux temperature after 6 days and 43 days, respectively. The other alkoxy derivatives were prepared at 25°C. As found with $LiAl(OCH_3)_3H$, $LiB(OCH_3)_3H$ underwent disproportionation to $LiB(OCH_3)_2H_2$ (solution H/Li = 2.5) and $LiB(OCH_3)_4$ (solid = 0.12) after ten hours at 25°C (1.0 M). Typical analyses for the alkoxy derivatives of $LiBH_4$ are presented in Table 2.

The benzene and THF solutions of tetrabutylammonium aluminum hydride (Bu_4NAlH_4) were prepared according to the method of Ehrlich and coworkers.[21] To prepare the THF solution, 80.0 millimoles of $NaAlH_4$ (40.0 ml of 0.400 M) in THF was added to 80.0 millimoles of tetrabutylammonium bromide (6.44 g) in THF. A precipitate formed slowly while the solution was stirred at 25°C for three days. The solid was filtered with difficulty in a dry box giving a colorless solution which contained less than 0.5% bromide. To prepare the benzene solution, 40.0 millimoles of $NaAlH_4$ (80.0 ml of 0.500 M) in THF was placed in a 250 ml flask. The THF was removed under vacuum, and a benzene solution of Bu_4NBr (20.0 millimole, 6.44 g) was added. The mixture was stirred at 25°C for 5 days, and NaBr and excess $NaAlH_4$ were then removed by filtration. The bromide content of the solution was not detectible as determined by Volhard titration.

The concentration of these stock solutions of hydrides was determined by at least two methods. Lithium and sodium were determined by

flame photometry, aluminum was determined by EDTA titration, and active hydride was determined by measuring evolved hydrogen from a hydrolyzed sample. Bromide was determined by the Volhard method.

Ebullioscopic Measurements

A detailed description of the apparatus and procedure for the ebullioscopic determination of apparent molecular weights is described elsewhere.[23] The measurements were performed in THF and diethyl ether at a pressure of 740 mm Hg.

Spectral Measurements

A Varian Model A-60A, 60 MHz, Nuclear Magnetic Resonance spectrometer was used for recording all NMR spectra. Tetramethylsilane was used as an internal standard for all measurements. Frequencies were measured by the side band technique with a Hewlett-Packard (Model 2000 D) oscillator and frequency counter (Model 5512 A), and were reproducible to within $\pm$ 0.2 Hz. Solutions were prepared in the dry box or on the bench top using Schlenk-type[20] techniques, and spectra were run immediately after preparation of the solutions.

A Perkin-Elmer Model 621 infrared spectrometer or a Beckman IR-12 spectrometer was used for recording the infrared spectra. Sodium chloride (0.1 mm) cells and potassium bromide (0.5 mm) matched cells were used. The transfer of solutions was accomplished on the bench top using Schlenk-type[20] techniques, and the spectra were recorded immediately after the preparation of the solutions.

Calculations

All pertinent calculations were performed on the RCA Spectra-70

Computer at Georgia State University. Several computer programs written in the basic computer language are presented in the Appendix.

CHAPTER III

RESULTS

Conductance

The equivalent conductances for THF solutions of $LiAlH_4$, $NaAlH_4$, Bu_4NaAlH_4, and $LiBH_4$ are presented in Tables 3-8. When free ions are present in equilibrium with ion pairs and triple ions, Fuoss[24*] has shown that the equivalent conductance of the solution is adequately represented by eq. 1 or 2 where K_a is the ion pair dissociation constant, Λ_o is the

$$\Lambda = \Lambda_o/(K_a C)^{\frac{1}{2}} + \lambda_o C^{\frac{1}{2}}/K_t(K_a)^{\frac{1}{2}} \qquad (1)$$

$$\Lambda = AC^{-\frac{1}{2}} + BC^{\frac{1}{2}} \qquad (2)$$

limiting equivalent conductance, λ_o is the limiting equivalent conductance of the triple ion, C is the concentration of the solute, and K_t is the triple ion dissociation constant. Consequently, a plot of log Λ vs. log C should be linear with a slope of -0.5 if only ion pairs are present in the dilute solution region. The plots are presented in Figure 2. For each hydride studied a concentration range was found for which a plot of log Λ vs. log C was linear with a slope of approximately -0.5 (5×10^{-4} M to 2×10^{-7} M). The Fuoss conductance equation 3, which describes

*The detailed derivation of all the pertinent Fuoss equations are presented in the Appendix, together with the respective computer programs required for the calculations.

$$F/\Lambda = 1/\Lambda_o + \gamma_{\pm}^2 C\Lambda/FK_a\Lambda_o^2 \qquad (3)$$

the equivalent conductance of ionic solutions when only ion pairs and free ions are present, was applied to the data. The values of the density, viscosity and dielectric constants for THF needed to apply the Fuoss equations to the data were obtained from the work of Hogen-Esch and Smid.[25] An initial approximation of Λ_o was made and an iterative procedure was employed to give the best least squares fit of the data to eq. 3. The values obtained in the last iteration are plotted in Figure 3, as F/Λ versus $C\Lambda\gamma_{\pm}^2/F$. From the intercept and slope determined from the least squares calculation, the infinite dilution equivalent conductance (Λ_o) and ion pair dissociation constant (K_a) are evaluated. The Λ_o and K_a values extracted in this manner from the conductance data are tabulated in Table 9. Considerable uncertainty exists for the intercepts, and the Λ_o and K_a values are therefore uncertain by at least $\pm$ 10%. However, Szwarz[26] and coworkers have shown that the Λ_o values for the Li^+, Na^+, and Bu_4N^+ ions are approximately identical in THF. Consequently the Λ_o values for the complex metal hydrides studied here should be approximately the same. Since this is observed, these results are consistent with previous investigations.

When the plots of log Λ versus log C are no longer linear, higher aggregates, such as the triple ion, probably begin to form. Fuoss[24] has developed equation (4) to describe the equivalent conductance of ionic solutions when triple ions and ion pairs are encountered.

$$\Lambda C^{\frac{1}{2}} g(C) = \Lambda_o K_a + (\Lambda_o K_a^{\frac{1}{2}}/K_t)(1 - \Lambda/\Lambda_o)C \qquad (4)$$

The triple ion dissociation constant, K_t, can be estimated from this equation. The data for each hydride studied has been fitted to equation (4) in the concentration range, 2×10^{-2} M to 6×10^{-4} M, where both triple ions and ion pairs are encountered. A plot of $\Lambda C^{\frac{1}{2}} g(C)$ vs. $(1 - \Lambda/\Lambda_o)C$ for $LiAlH_4$, $NaAlH_4$, Bu_4NAlH_4 and $LiBH_4$ is presented in Figure 4. Since the plots are linear with a correlation coefficient of at least 0.99, it appears that eq. 4 adequately describes the data and that triple ions are forming in the solutions of all the hydrides studied. In order to calculate K_t from the slope a value of the infinite dilution equivalent conductance (λ_o) of the triple ion is required. An approximate value[24] for this quantity is taken to be 1/3 of Λ_o because the triple ion is a cluster of free ions. The K_t values are also presented in Table 9. A minimum is observed in the equivalent conductance curves for these hydrides. Above the minimum the data show a positive deviation from eq. 4. As the concentration is increased, the conductance value for these hydrides increases to a maximum at approximately one molar.

Temperature dependent studies were performed on a separate set of $LiAlH_4$ and $NaAlH_4$ solutions between 25°C and -75°C (Tables 10-12). The Fuoss equations were applied to the data to obtain a consistent set of K_a values at each temperature. A plot of log K_a versus 1/T for both hydrides is shown in Figure 5. A linear plot is observed for $LiAlH_4$ and the enthalpy of dissociation is estimated to be -2.2 kcal/mole ($\pm$ 0.5). In the plot for $NaAlH_4$ considerable curvature is observed, but the curve

can be resolved into two component lines giving ΔH_d° values of -0.6 and -5.6 kcal/mole ($\pm$ 0.5) respectively.

The equivalent conductances for $LiAl(OCH_3)_3H$ and $LiAl(Ot\text{-}Bu)_3H$ in THF are presented in Tables 13-14. The equivalent conductance for these hydrides is independent of the concentration over a wide concentration range, in contrast to the hydrides previously discussed. The equivalent conductance for a 0.1 M solution of $LiAl(OCH_3)_3H$ in THF is approximately the same as a 0.1 M solution of $LiAlH_4$ in the same solvent, while the equivalent conductance of a 0.1 M solution of $LiAl(Ot\text{-}Bu)_3H$ in THF is approximately the same as a 0.1 M solution of $LiBH_4$ in the same solvent. The equivalent conductances of diethyl ether solutions of $LiAlH_4$ and $LiBH_4$ (Table 15) are extremely small and concentration independent.

Ebullioscopic

The apparent molecular weights of the complex metal hydrides were determined near the boiling point of the solvent between 0.05 m and 0.6 m. The calculated i-values defined as the ratio of the experimentally determined molecular weight and the formula weight are shown in Figures 6,7, and 8 as a function of concentration.

The association curves for $LiAlH_4$, $NaAlH_4$ and $LiBH_4$ are shown in Figure 6. In THF, both $LiAlH_4$ and $NaAlH_4$ have i-values of 1.0 in dilute solution, increasing with increasing concentration to a limiting value of 1.8. In diethyl ether, $LiAlH_4$ has significantly higher i-values over the same concentration range. $NaAlH_4$ is insoluble in diethyl ether and ebullioscopic data could not be obtained. The i-values for $LiBH_4$ in THF are approximately constant at 1.5 over the entire concentration range. In

diethyl ether, the i-values of $LiBH_4$ are higher at all concentrations, increasing from 1.7 in dilute solution to 2.3 at the highest concentrations.

At 0.05 m an i-value of approximately 1.0 is predicted from the conductance data for $LiAlH_4$ and $NaAlH_4$ in THF, which is in good agreement with what is found. At the higher concentrations the conductance data indicate that the triple ions are the predominant species in solution, i.e., the i-value should approach a limiting value of 1.5. For $LiBH_4$ in THF the conductance data show that this hydride is considerably more associated than either $LiAlH_4$ or $NaAlH_4$ at 0.05 m, and the calculated i-value from conductance data is approximately 1.4 at 0.05 m. Since the conductance and ebullioscopic data are consistent at 0.05 m, it is unlikely that any species other than ion pairs and triple ions are present in this concentration range. However, activity coefficients have been taken into account only in the conductance data calculations and predicted i-values. Since it is impossible at this time to correct the ebullioscopic data for activity coefficients, larger aggregates cannot be completely ruled out as possibilities at higher concentrations.

$LiAl(OCH_3)H_3$ in THF has an association curve which is almost identical to that found for $LiAlH_4$. $LiAl(Ot\text{-}Bu)H_3$ and $LiAl(OCHPh_2)H_3$ have identical association curves with i-values varying from 1.0 to 1.3. The trisubstituted derivatives, $LiAl(Ot\text{-}Bu)_3H$ and $LiAl(OCHPh_2)_3H$, have a constant i-value of 1.0 from 0.05 to 0.4 m showing only a slight decrease at the higher concentrations. The association curves for $LiAl(OCH_3)_2H_2$ and $LiAl(OCH_3)_3H$ are substantially different than the curves found for

the other hydrides shown in Figure 7 and 8. At the most dilute concentrations, the i-values are 1.0 and 1.5 respectively, rising sharply to 2.5 and 2.8 at the higher concentrations.

The association curves for the corresponding alkoxy derivatives of $LiBH_4$ in THF are presented in Figure 8. The methoxy derivatives of $LiBH_4$ exhibit association curves which are similar to those found for the methoxy derivatives of $LiAlH_4$. For the remaining derivatives of $LiBH_4$, the i-values are all below 1.0 and almost constant in the concentration range studied.

All the alkoxy derivatives of $LiAlH_4$ and $LiBH_4$ are insoluble in diethyl ether, and ebullioscopic data could not be obtained.

NMR Studies

The chemical shift of the α-methylene hydrogens of THF was monitered as a function of the mole ratio of THF to lithium salt dissolved in diethyl ether (Figure 9). In the absence of salt, the chemical shift of THF remained constant at 218.5 Hz over the range of concentration of THF used in this study. In the presence of 0.3 M $LiAlH_4$ a change in the chemical shift of THF was observed, while the chemical shifts of the diethyl ether hydrogens remained constant. The chemical shift decreased as the mole ratio of salt increased, until the chemical shift approached that value found in pure THF. At a mole ratio of THF to $LiAlH_4$ of 4:1, a change in the slope was observed, indicating the existence of a stable four-coordinated species, i.e., $LiAlH_4 \cdot 4THF$. A similar result was obtained for lithium perchlorate and lithium iodide. However, the tetra-

butylammonium aluminum hydride did not cause the chemical shift of the α-methylene hydrogens to change in this concentration region. Consequently the change observed for $LiAlH_4$ must be attributed to the lithium ion exclusively. The most reasonable explanation for these results is to view the lithium ion in THF as specifically solvated by four molecules of THF. $NaAlH_4$ does not have an appreciable solubility in diethyl ether; it was thus not possible to perform corresponding experiments on other sodium salts. Previous workers have performed similar experiments with lithium salts in acetone-nitromethane[27] mixtures, dimethylformamide-dioxane[28] mixtures, and 2-pyrrolidone-dioxane[29] mixtures. In each case the carbonyl oxygen formed a four-to-one solvate with the lithium ion. Apparently four ligands are the maximum number which can be placed in the first coordination sphere of the lithium ion.

A similar experiment for $LiBH_4$ in THF-diethyl ether mixtures does not show a break at a mole ratio of THF to lithium of 4:1 as was found with $LiAlH_4$, but shows a plateau at a mole ratio of 1:1 with a gradual change in chemical shift thereafter. Apparently there is less specific solvation of the lithium ion by THF. This is consistent with the low conductance and higher association values found for $LiBH_4$ in THF.

The NMR spectra of 0.1 M and 1.0 M THF and diethyl ether solutions of $LiAlH_4$ were recorded 1000 Hz upfield and downfield from TMS. No signals which could be attributed to the hydrogens were found. The NMR spectrum of $LiAlH_4$ in completely deuterated ($THF\text{-}d_8$) solvent was also recorded, but no hydrogen signal was found. Since the aluminum has a spin of 5/2, the expected sextet is apparently lost in instrument noise because of extensive broadening due to the nuclear quadrupole moment of

aluminum. An extremely broad aluminum-27 signal (420 Hz) is reported by Haraguchi and Fujiwara[14] for $LiAlH_4$ in diethyl ether. The broadening of the signal is also attributed to unresolved hyperfine splitting which is produced by the four protons bonded directly to the metal.

Spectral

New absorption bands appear in the infrared spectra of 0.1 M THF solutions of $LiClO_4$, LiI, LiBr and $LiAlH_4$ near 420 cm^{-1}, which are not present in pure THF. These spectra are shown in Figure 10. Two closely spaced absorptions are evident for $LiClO_4$, LiI and LiBr near 420 cm^{-1}. $LiAlH_4$ has a much broader absorption in this region with three peaks clearly evident. The most intense band occurs at 450 cm^{-1} for $LiAlH_4$, but the two bands near 420 cm^{-1} are also present. Previous workers[30] have found similar bands for LiI, LiBr, and LiCl in THF at 373 cm^{-1}, 378 cm^{-1}, and 387 cm^{-1}, respectively, which have been attributed to the vibration of the lithium ion in a solvent cage. The new bands that appear in this study can also be attributed to a vibration of the lithium ion attached to the four THF molecules that are specifically solvated. These findings are consistent with the NMR results. Extreme care was taken to remove trace quantities of water and the concentration of the salts are much larger than the estimated concentration of water (0.001 M) present in freshly distilled THF. In the case of $LiAlH_4$, it is unlikely that any water is present. Two of the bands found in $LiAlH_4$ agree well with those for the other salts. Consequently, it is possible that the 50 cm^{-1} difference between the results shown in Figure 10 and the results of the previous workers is primarily due to their solutions containing

appreciable quantities of water. This conclusion is further substantiated by Dantel and Zeil[31] who report bands for $LiAlH_4$ in THF at 426 and 416 cm^{-1}. The higher frequency band at 450 cm^{-1} observed only for $LiAlH_4$ is possibly due to an interaction of the AlH_4^- ion with the oxygen of one of the THF solvate molecules. At 0.5 M the spectrum of $LiAlH_4$ in THF consists of two bands of approximately equal intensity at 455 and 440 cm^{-1} with a shoulder of diminished intensity at 420 cm^{-1}. The conductance and ebullioscopic results indicate that the predominant species present at 0.1 M and 0.5 M changes from ion pair to triple ion, and it is not surprising that spectral changes accompany this transformation.

In contrast to the lithium salts previously discussed, $LiBH_4$ in THF does not show a well defined band near 420 cm^{-1} in the infrared region which can be attributed to the vibration of the lithium ion in a solvent cage. This is consistent with less specific solvation of the lithium ion in THF solution of $LiBH_4$ which is indicated by the NMR mole ratio studies, conductance and ebullioscopic studies.

Spectral studies were also performed on THF solutions containing $LiClO_4$ and acetone at several mole ratios. As the ratio of lithium salt to acetone increased, the carbonyl band of acetone shifts to lower wave numbers (Figure 11). At a mole ratio of 14:1 when the concentration of acetone is 0.02 M, the shift reaches a maximum value of 7 cm^{-1}. A similar result is observed for acetone in diethyl ether (Figure 12). Apparently the ether solvate molecules bonded to the lithium ion can be readily replaced in the first coordination sphere by carbonyl compounds.

The observed band maxima found in the infrared spectra in the aluminum-hydrogen stretching and bending vibrational regions for the

several of the alkoxy derivatives of $LiAlH_4$ are presented in Table 35. A shift in the stretching band maxima to higher wave numbers (70 cm^{-1}) is observed for the mono- and tri-t-butoxy derivatives, while a shift of 110 cm^{-1} is observed for $LiAl(OCHPh_2)_3H$. The other derivatives show approximately the same absorption band as $LiAlH_4$ (1690 cm^{-1}). The boron-hydrogen stretching vibrational maxima for several of the alkoxy derivatives of $LiBH_4$ are presented in Table 36. Except for $LiB(Ot\text{-}Bu)_3H$ which has an absorption band at 2260 cm^{-1}, all the other borohydrides have an absorption band at 2220 cm^{-1}.

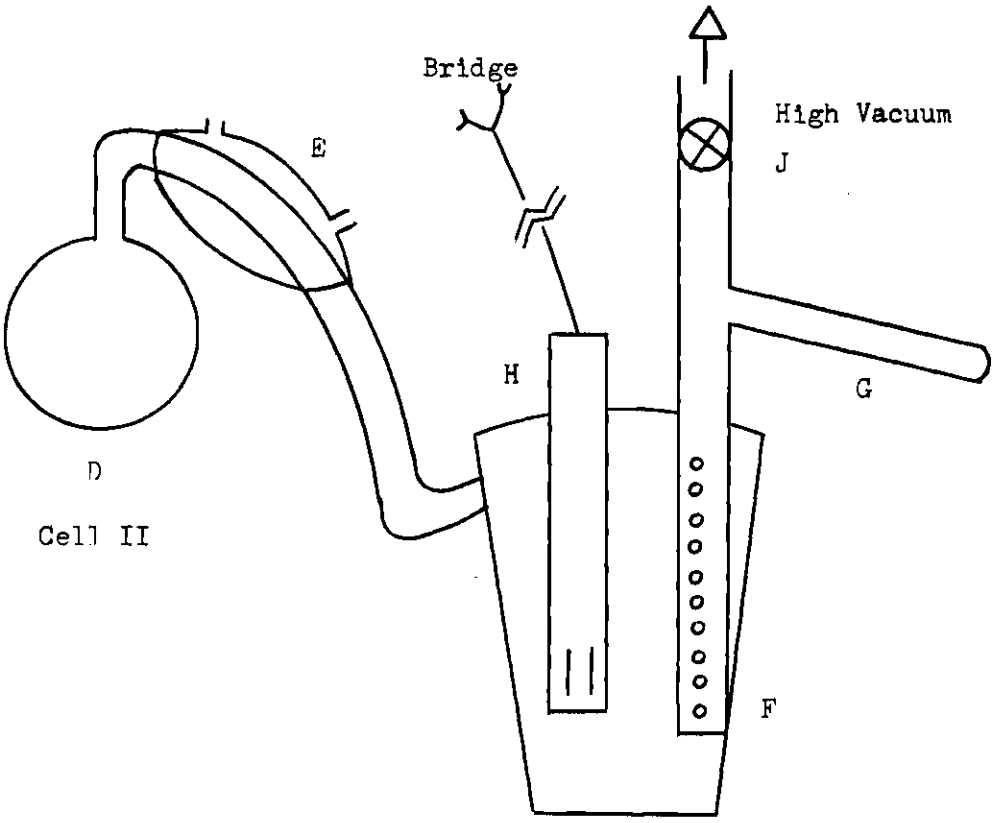

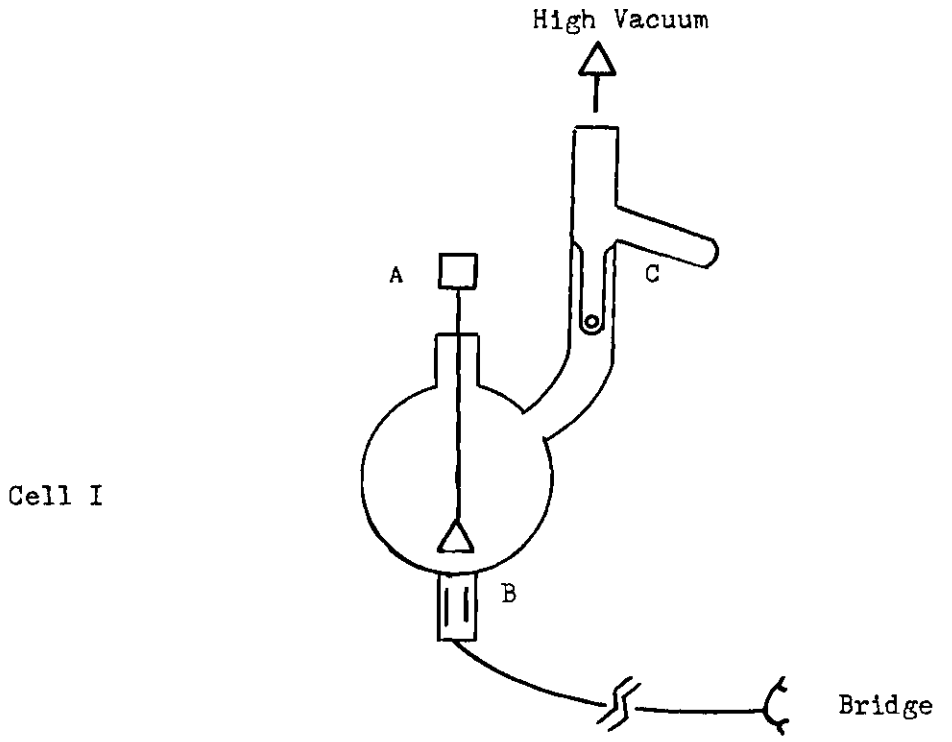

Figure 1. Conductance Cells.

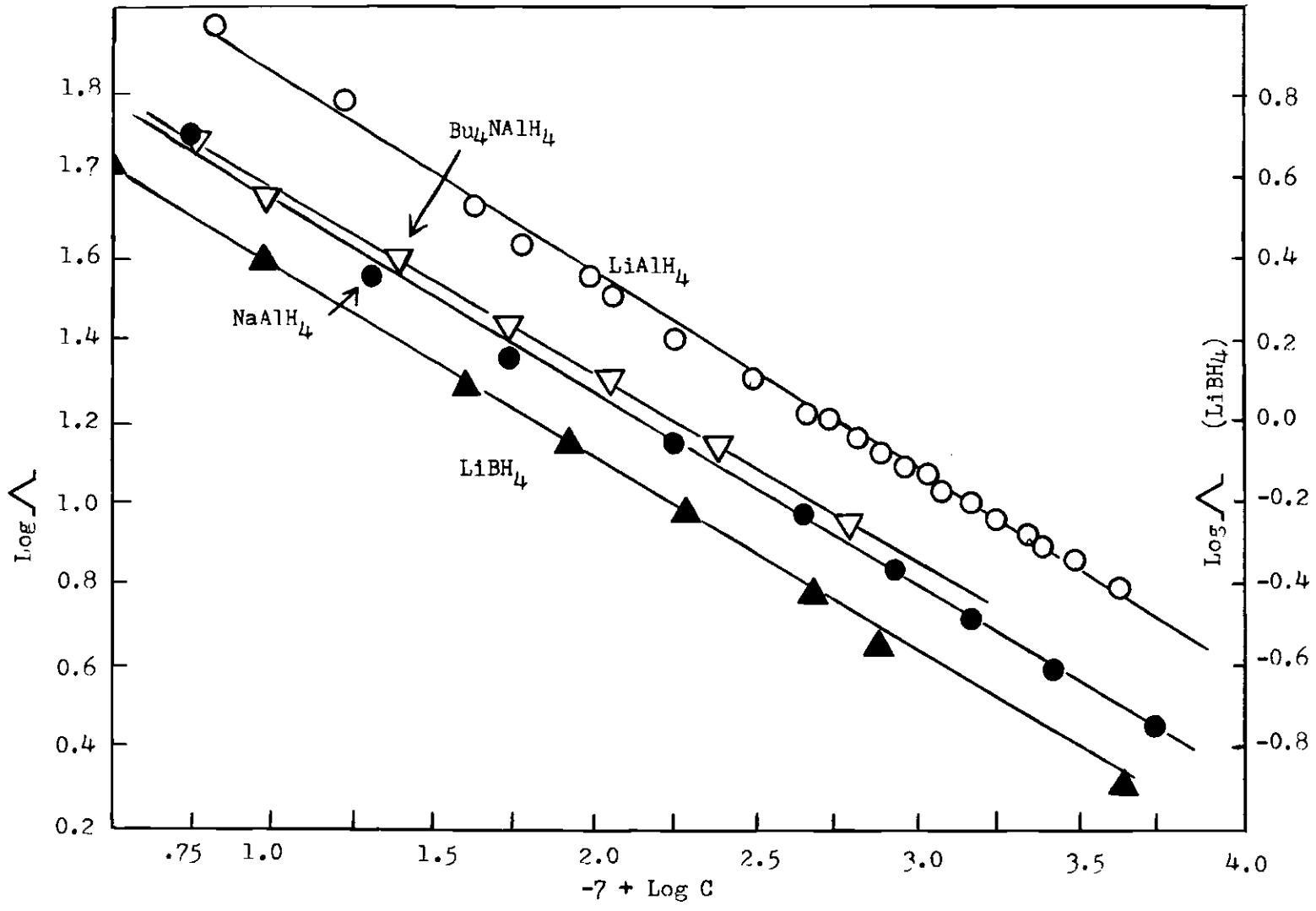

Figure 2. A Plot of Log Λ vs. Log C for $LiAlH_4$, $NaAlH_4$, Bu_4NAlH_4 and $LiBH_4$ in THF.

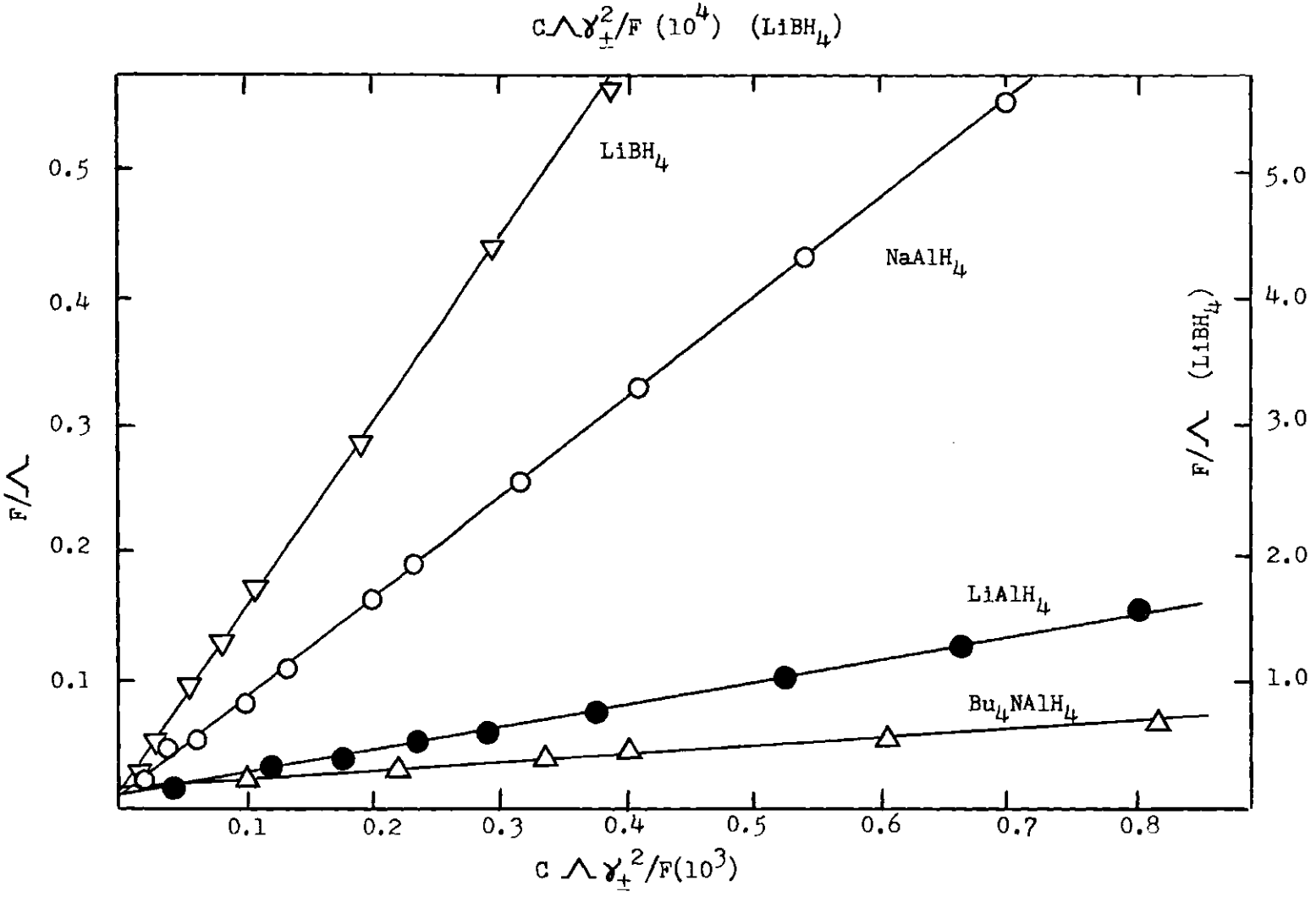

Figure 3. Fuoss Plots for $LiAlH_4$, $NaAlH_4$, $BuNAlH_4$ and $LiBH_4$ in THF at 25°C.

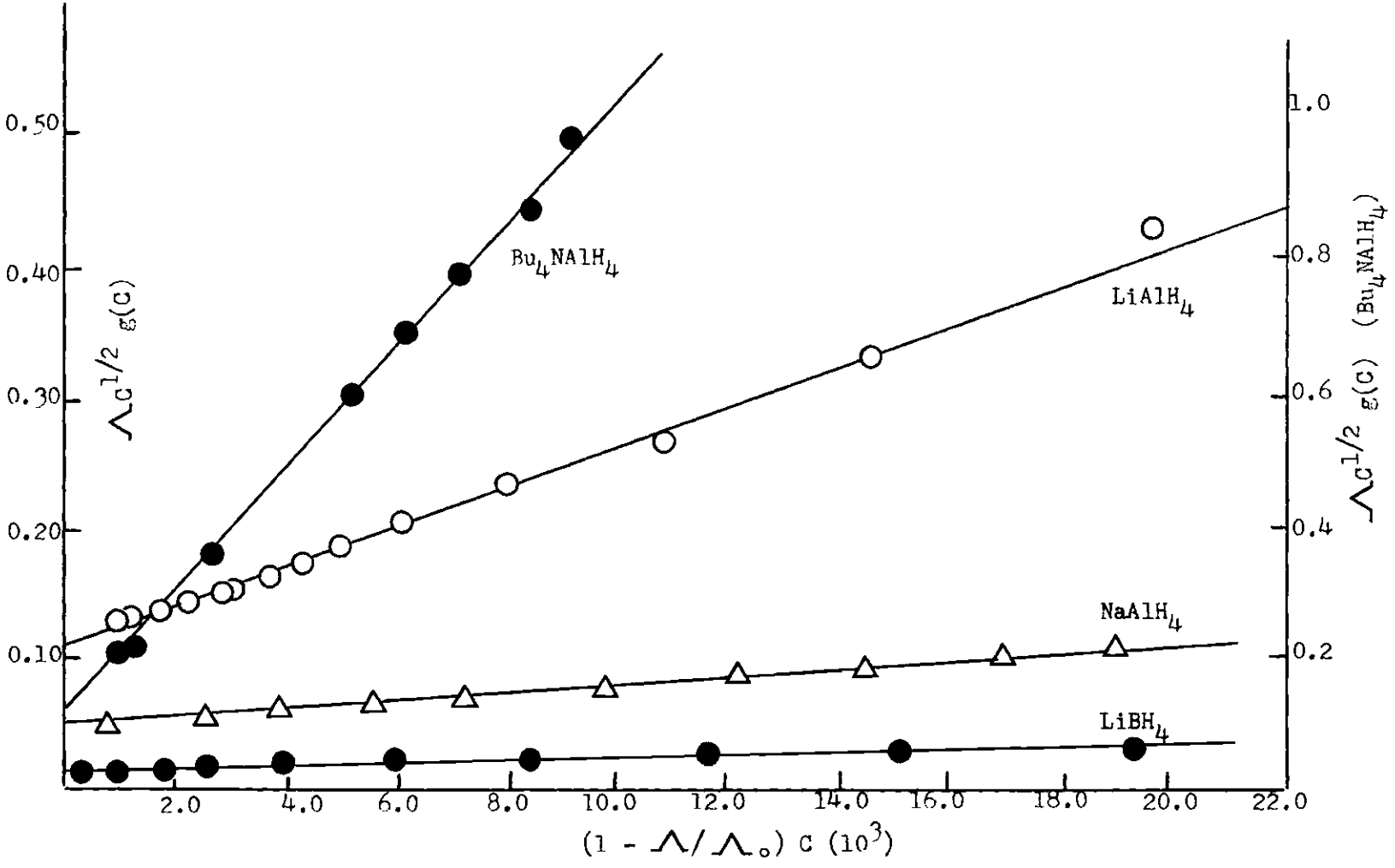

Figure 4. A Plot of Data in the Region of the Minimum for $LiAlH_4$, $NaAlH_4$, Bu_4NAlH_4 and $LiBH_4$.

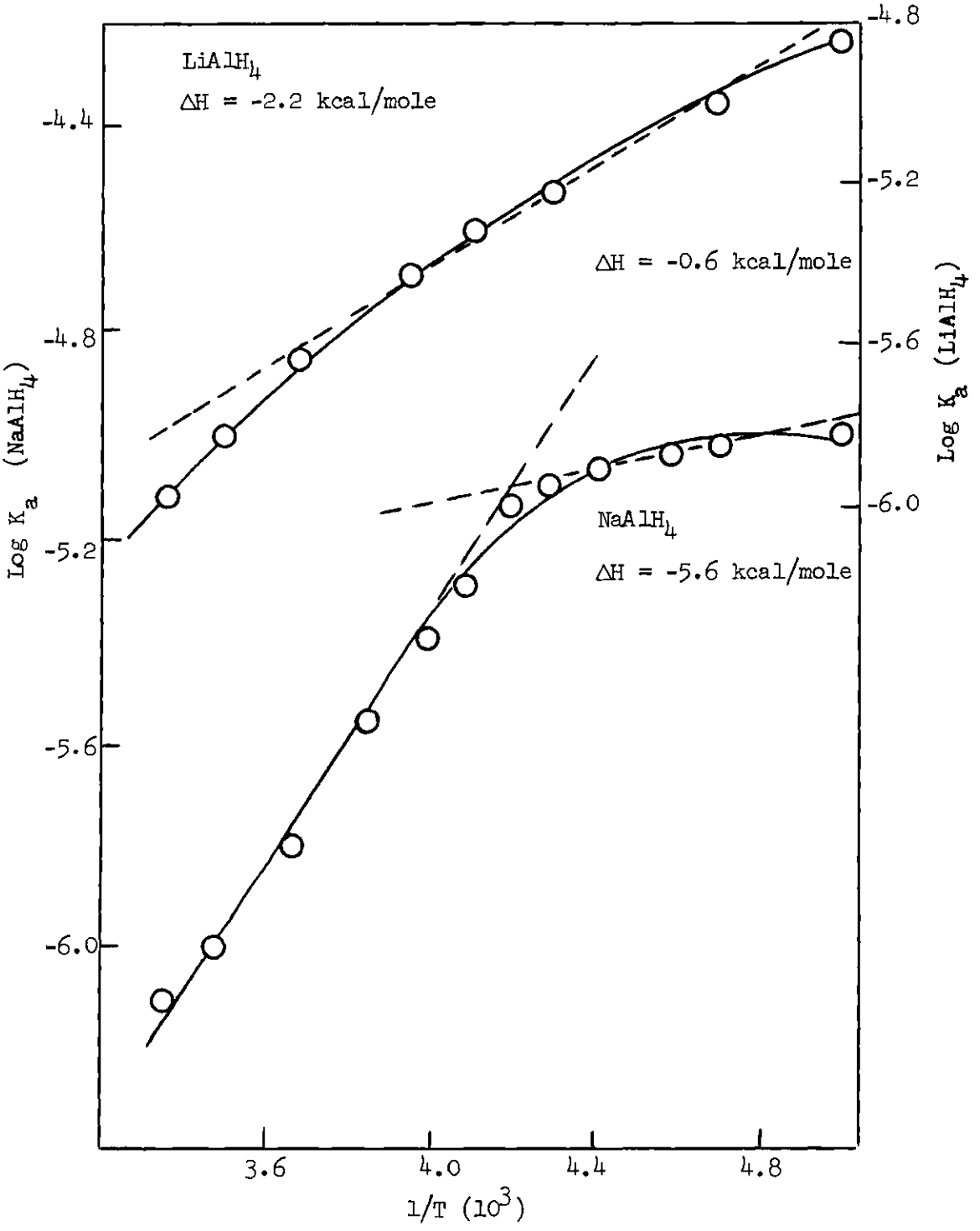

Figure 5. Temperature Dependence of the Dissociation Constants for $LiAlH_4$ and $NaAlH_4$ in THF.

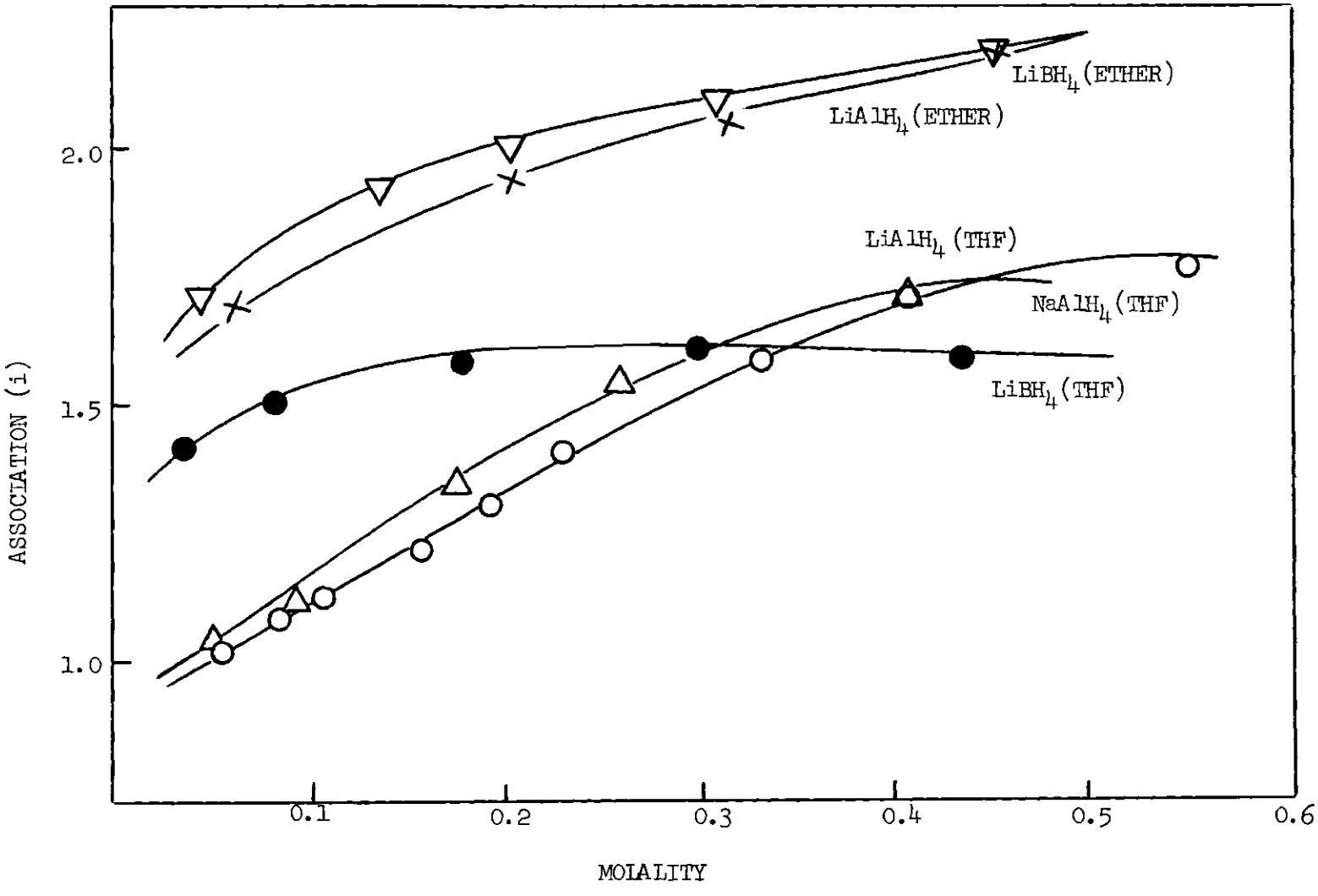

Figure 6. The Association of $LiAlH_4$, $NaAlH_4$ and $LiBH_4$ in Ethereal Solvents.

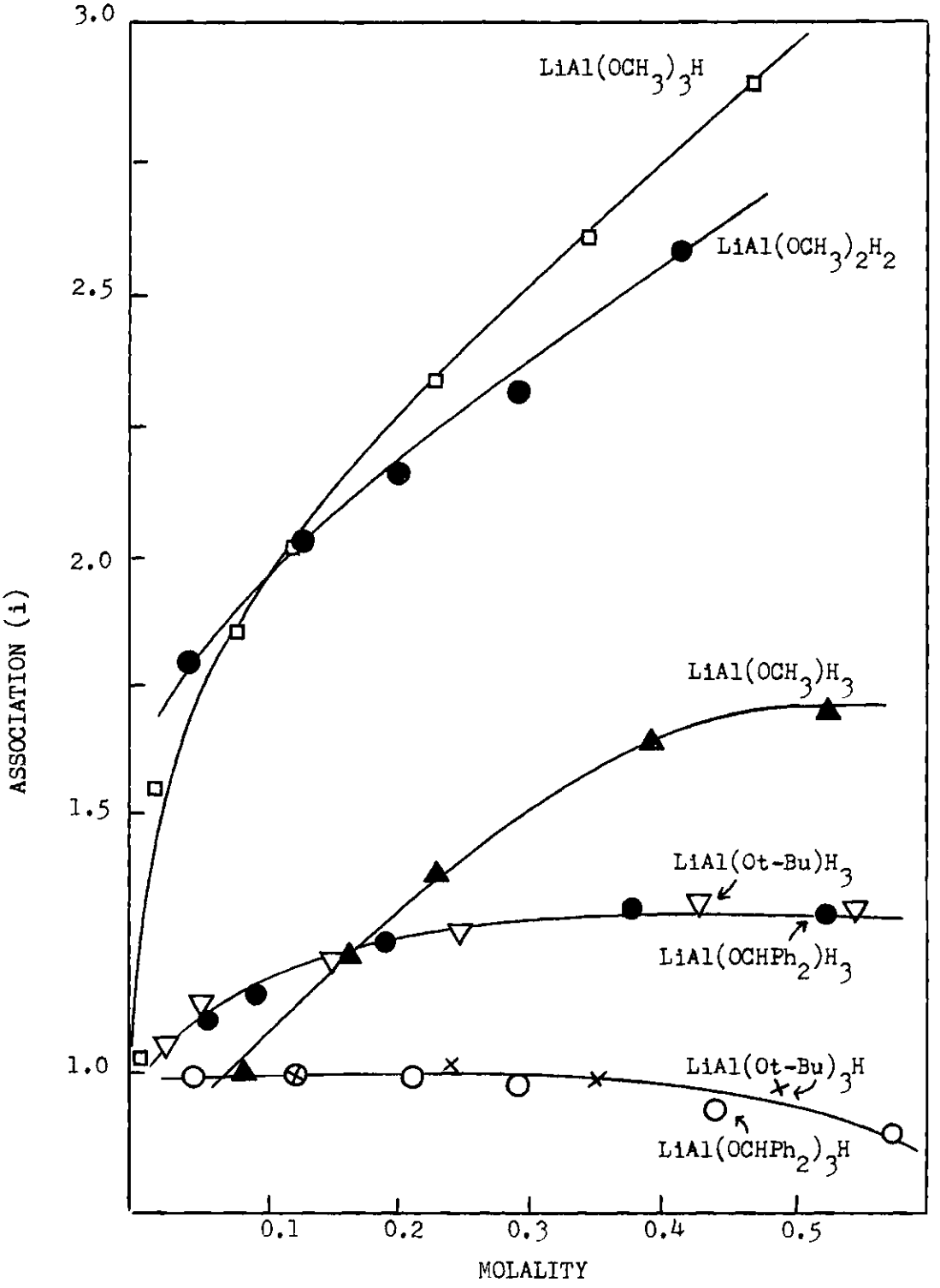

Figure 7. The Association of Several Alkoxy Derivatives of $LiAlH_4$ in THF.

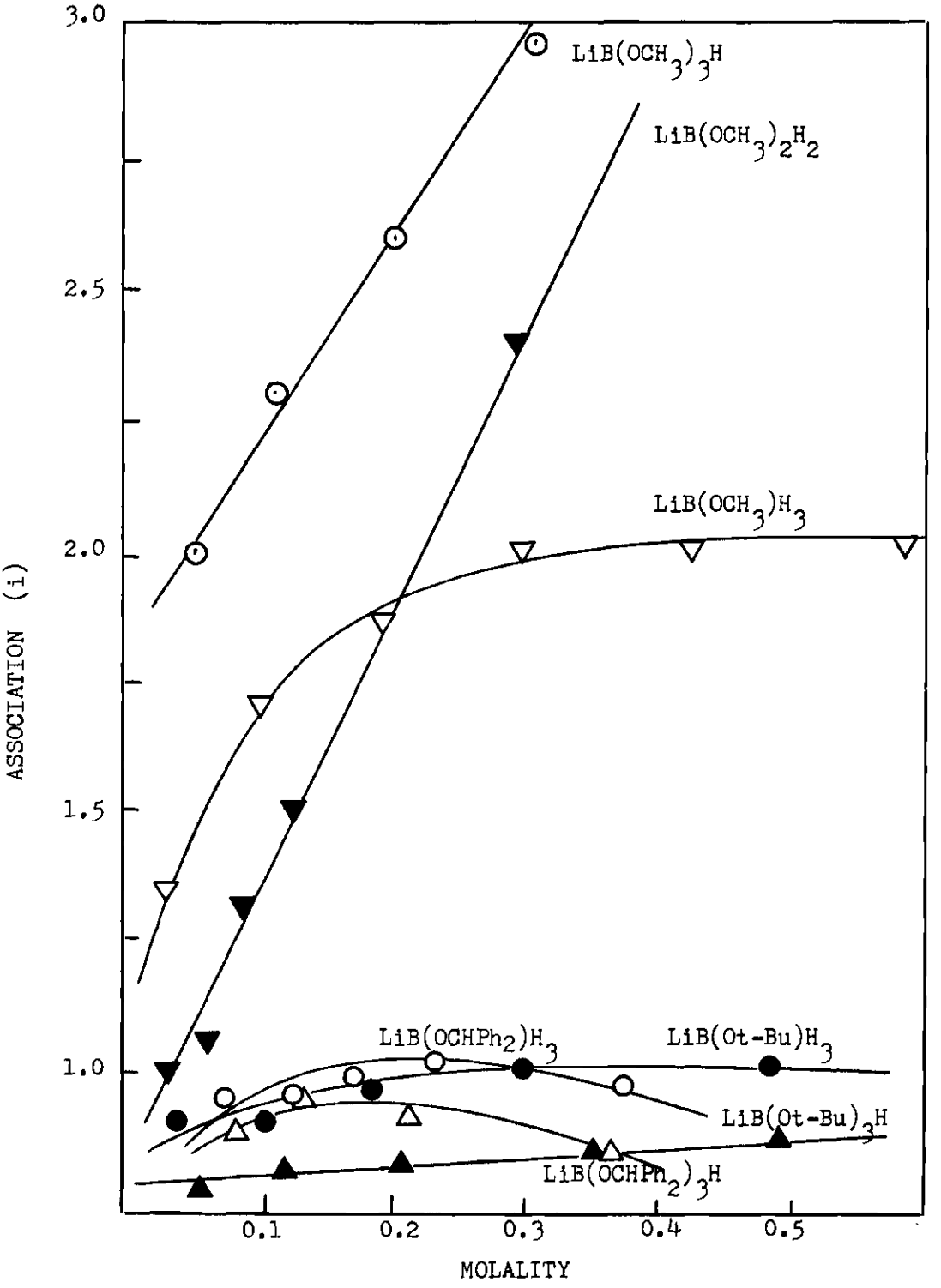

Figure 8. The Association of Several Alkoxy Derivatives of $LiBH_4$ in THF.

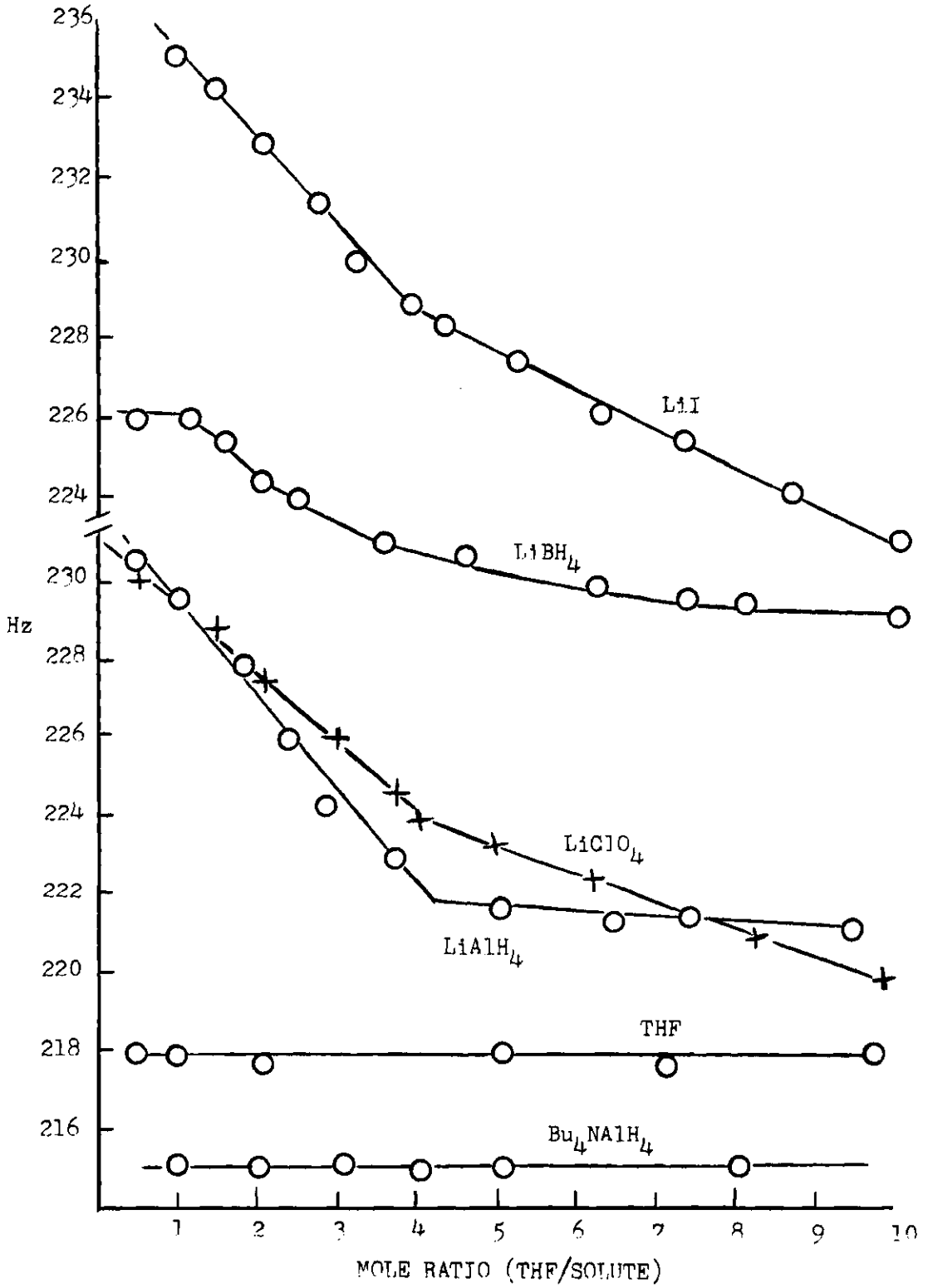

Figure 9. Chemical Shift of the THF Methylene Proton Signals as a Function of the Mole Ratio THF to Salt in Diethyl Ether.

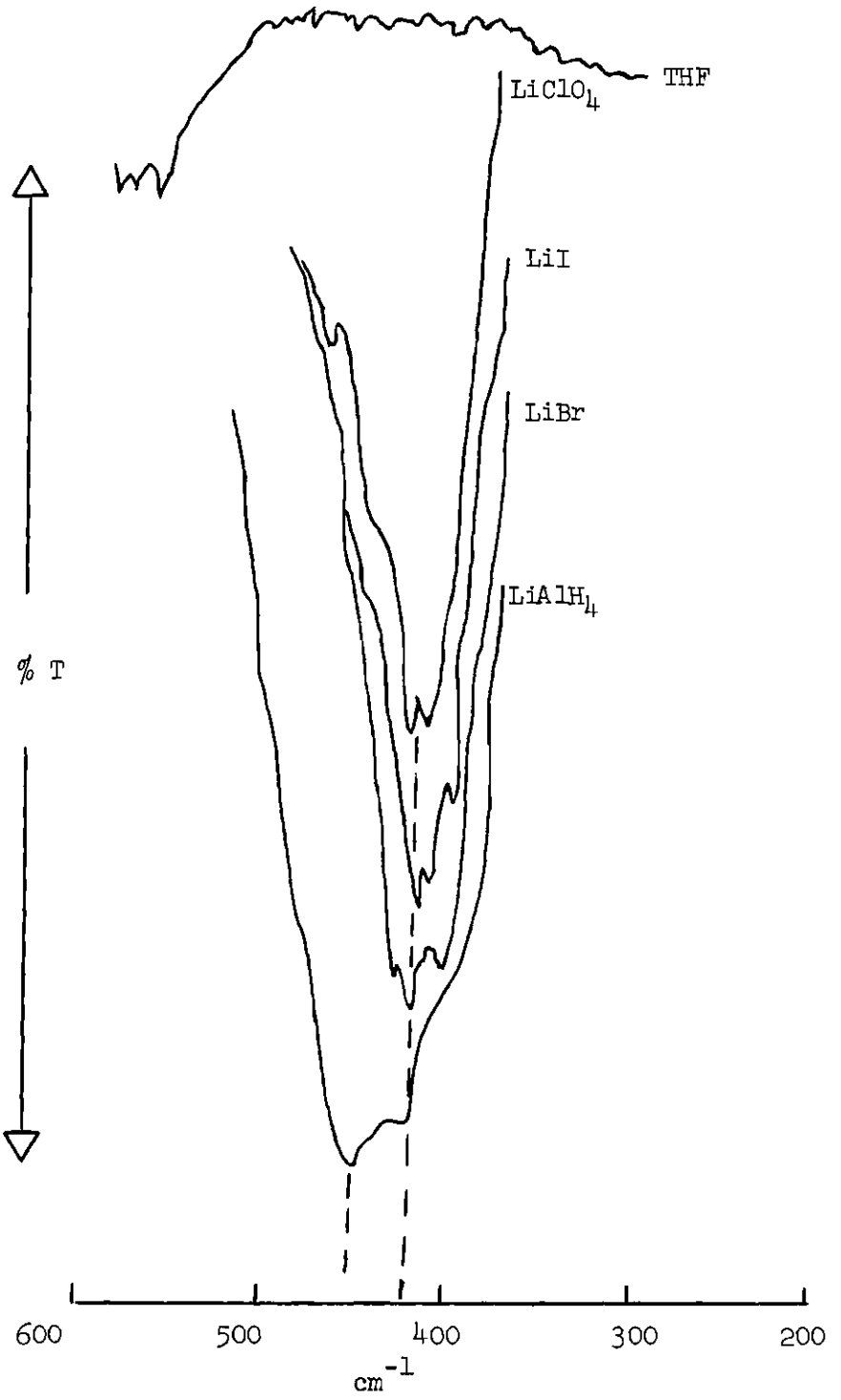

Figure 10. Infrared Spectra for Several Lithium Salts in THF. (Conc. $\simeq$ 0.1 M)

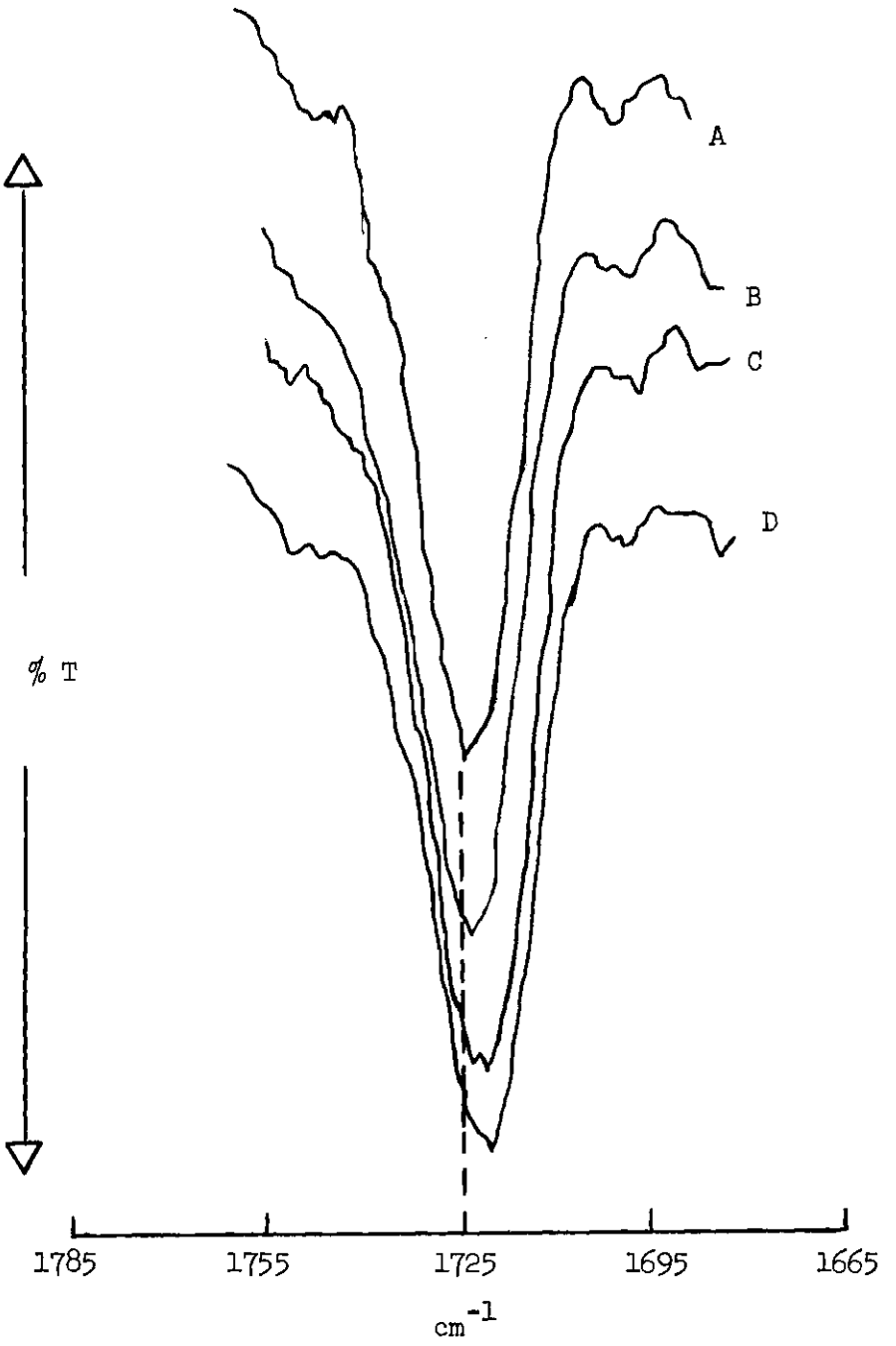

Figure 11. Spectra of Solutions of Acetone and $LiClO_4$ in THF. A, 0.02 M Acetone; B, $LiClO_4$:Acetone = 2:1; C, $LiClO_4$:Acetone = 4:1; D, $LiClO_4$:Acetone = 10:1.

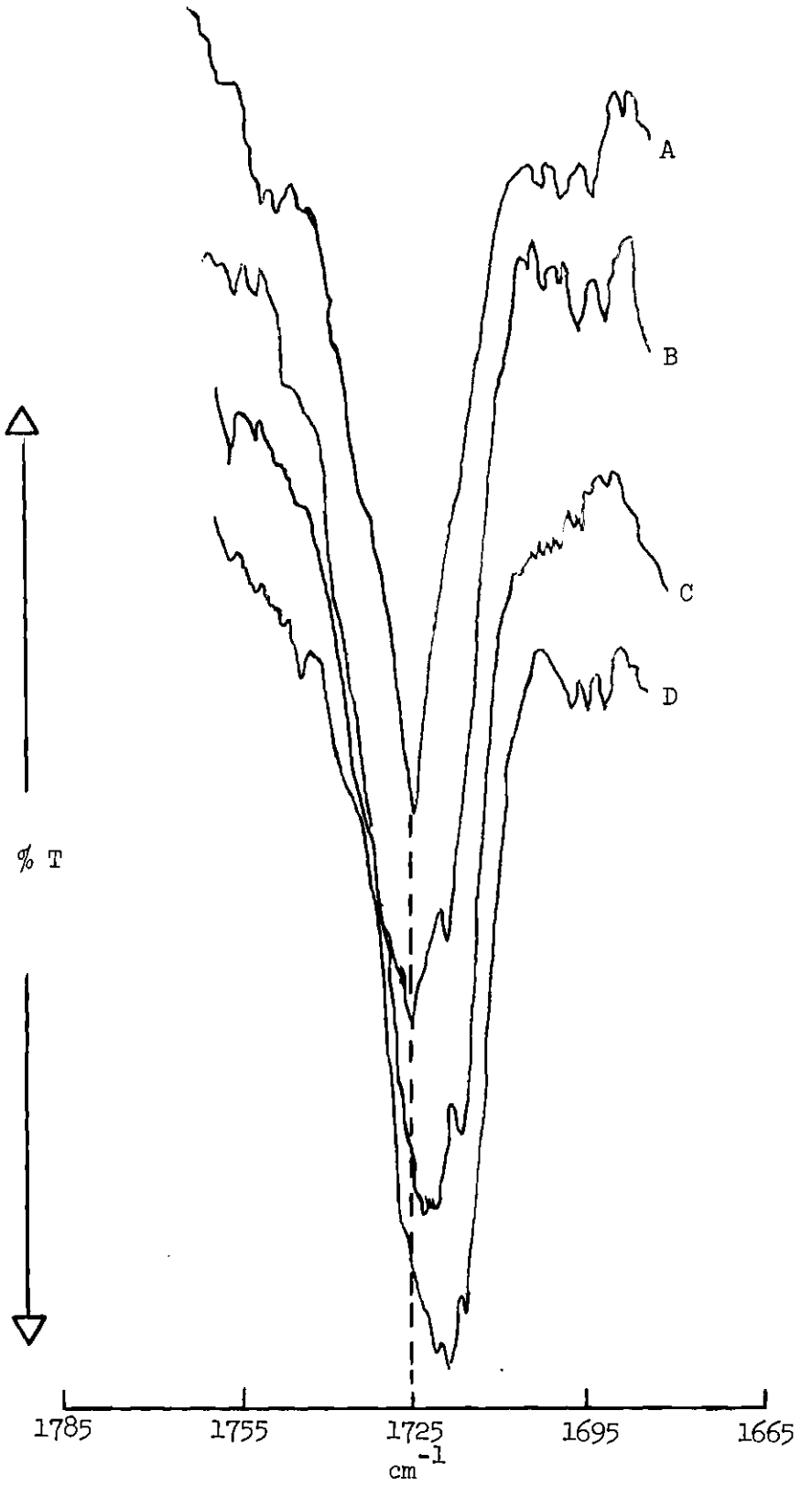

Figure 12. Spectra of Solutions of Acetone and $LiClO_4$ in Diethyl Ether. A, 0.023 M Acetone; B, $LiClO_4$:Acetone = 2:1; C, $LiClO_4$:Acetone = 6:1; D, $LiClO_4$:Acetone = 10:1.

CHAPTER IV

DISCUSSION AND CONCLUSIONS

Complex metal hydrides behave as weak electrolytes in THF. The conductance data for $LiAlH_4$, $NaAlH_4$, Bu_4NAlH_4 and $LiBH_4$ in THF are consistent with the presence of free ions and ion pairs in dilute solution, and the formation of triple ions as the concentration is increased. Two types of ion pairs are possible: (1) solvent separated ion pairs in which one of the ions is completely solvated by solvent, but the ions remain in close proximity, and (2) contact ion pairs in which a portion of the inner solvation sphere of the ions is removed and the ions are in intimate contact in the ion pair. If several spheres of solvation separate the ions, then the ions are considered to be free ions. Higher aggregates are also possible. The triple ions are clusters of three ions, and two types are possible, e. g., $LiAlH_4Li^{+1}$ or $AlH_4LiAlH_4^{-1}$. It is probable that the specific solvation in the ion pair and triple ion are the same. Hence if the solution contains solvent separated ion pairs, the triple ions should also be solvent separated, whereas if the solution contains both solvent separated and contact ion pairs, the triple ions should be a mixture of both types.

From the K_a and K_t values derived from the conductance data, the fraction of each species present at a particular concentration can be calculated from the equilibrium expressions, the mass balance requirement and the extended Debye-Hückel relationship for the activity coefficients of

the ions. From these values an i-value can be calculated which agrees within experimental error with those found in the ebullioscopic experiments at 0.05 M for $LiAlH_4$ and $LiBH_4$, establishing that the $LiAlH_4$ ion pair and the $LiBH_4$ triple ion are predominant species present in solution at this concentration. For concentrations greater than 0.05 M, the calculations break down. Since the association curves for $LiAlH_4$ and $NaAlH_4$ reach an i-value plateau at approximately 1.5 and the association curve for $LiBH_4$ is essentially constant at 1.5, it is evident the triple ion is the predominant species present in solution at the higher concentrations. The formation of triple ions in these systems is to be expected, since it is well established[37] that in solvents of dielectric constant less than 12, triple ions usually occur. From the conductance data it is impossible to distinguish between the two possible triple ions, e.g., $[LiAlH_4Li]^{+1}$ and $[AlH_4LiAlH_4]^{-1}$. The ebullioscopic data indicate, however, that equal amounts of both triple ions are probably formed.

The simplest model of an electrolyte solution assumes the ions to be charged spheres, with radii equal to that found in the crystal, distributed in a solvent continuum characterized by the macroscopic dielectric constant and viscosity. Using this model, Fuoss[24] demonstrated that the K_a for ion pairs is represented by eq. 5 where D is the macro-

$$K_a = (3000/4\pi r^3 N) \exp(-e^2/rDkT) \qquad (5)$$

scopic dielectric constant, r is the center-to-center distance between the ions, and the remaining symbols have their usual meaning. Using the

measured K_a values and the dielectric constant at 25°, eq. 5 was solved numerically to give a value for the center-to-center distance between the ion pairs. The center-to-center distances for each ion pair derived from eq. 5 are presented in Table 37, in comparison with values estimated from crystalligraphic parameters and the Dreiding models proposed for the ion pair. It was assumed that the four solvate THF molecules are tetrahedrally arranged around the lithium and sodium ions in the models and that the Bu_4N^+ ion was not specifically solvated. The closest distance of approach of the AlH_4^- ion to the solvated lithium or sodium ions was via attachment of one of the hydrogens to an oxygen of a THF molecule. This conclusion is supported by the appearance of a band in the infrared spectrum of $LiAlH_4$ at 450 cm^{-1}, which did not occur in the spectra of the other lithium salts. For $LiAlH_4$ this model is in perfect agreement with the center-to-center distance derived from the K_a via eq. 5. In $NaAlH_4$, the value predicted by the model is also reasonably close. Consequently, these comparisons strongly suggest that the ion pairs are solvent separated at 25°C. This conclusion is consistent with the NMR studies by Schaschel and Day,[33] and the infrared spectral interpretation of the new bands in the THF solutions. When the radius calculated from the Dreiding model of the ion pair of Bu_4NAlH_4 with the two ions in close proximity is compared to the value derived from eq. 5, an almost perfect agreement is obtained. The center-to-center distance predicted from the crystal radii is also very close to the value found for $LiBH_4$ in close proximity. It is expected that the Bu_4NAlH_4 would exist as a contact ion pair in THF solution, since no specific solvation is observed in the NMR studies. However, solvation of the lithium ion should occur for

$LiBH_4$ as well as $LiAlH_4$. Some forces must, therefore, exist in the contact species of $LiBH_4$ that compensate for the loss of solvation energy of the lithium ion. It is possible that the $LiBH_4$ ion pair has appreciable covalent character, since the differences observed for $LiBH_4$ and $LiAlH_4$ cannot be due to the slight change in the size of the anions.

An analysis of the available thermodynamic data for the dissociation of ion pairs in THF by Hogen-Esch and Smid[25] has established that the enthalpy of dissociation for the contact ion pair is approximately -8 to -10 kcal/mole for salts that are specifically solvated at the cation. On the other hand, the enthalpy of dissociation for a solvent separated ion pair should be -1 to -2 kcal/mole. Furthermore, if there is little change in specific solvation of the ion pair during the dissociation process, the enthalpy of dissociation (ΔH_d°) will be represented by expression (6) derived from the continuum model. Since dlnD/dlnT is

$$\Delta H_d^\circ = (Ne^2/rD)\left[1 + d\ln D/d\ln T\right] \qquad (6)$$

calculated from the temperature dependence of the dielectric constant to be -1.20 at 25° , the ΔH_d° predicted by the continuum model for $LiAlH_4$ is -0.8 kcal/mole. This is in reasonable agreement with the observed value for the $LiAlH_4$ solvent separated ion pair.

On dissociation of the solvent separated ion pair, the solvated ion carries its solvation shell with it. Any specific solvation enthalpy is therefore small and the ΔH_d° value can be calculated from eq. 6. However, the slightly larger negative value of ΔH_d° that is observed may be genuine and could be an indication that additional solvation occurs on

dissociation of the solvent separated ion pair. On dissociation of the contact ion pair, an increase in the specific solvation must occur especially where strong specific solvation effects are present. The large negative value for the enthalpy of dissociation is expected and is to a large extent caused by the strong gain in solvation enthalpy on formation of the solvent separated ion pair from contact ions. In this process, the solvating power of the solvent rather than its macroscopic dielectric constant is of prime importance. Furthermore, the increase in enthalpy may be due to an increase in the average number, but not necessarily integral number of solvent molecules in the solvation sphere about the cation.

Since the plot of log K_a vs. $1/T$ is not linear, it is not possible to unambiguously derive an enthalpy of dissociation for the ion pair of $NaAlH_4$. The pronounced curvature of this plot can be interpreted[25] as indicative of the presence of both contact and solvent separated ion pairs in equilibrium with free ions. Between -30 and -70°C the points can be fitted to a least squares line with a slope corresponding to a ΔH_d° = -0.6 kcal/mole. This value is consistent with the presence of predominantly solvent separated ion pairs. As the temperature is increased, the contact species are favored by the increase in kinetic energy of the solvent molecules, causing the equilibrium between the two types to shift toward the contact species. Consequently, the ΔH_d° = -5.6 kcal/mole derived from the slope of the curve between 25° and -15°C suggests that an appreciable fraction of the $NaAlH_4$ ion pairs exist in solution as contact species. When the contact ion pair dissociates to free ions, the cation must add at least one molecule of THF to its inner

solvation sphere, leading to the evolution of the extra quantity of energy not observed during the dissociation of a solvent separated ion pair. The difference in the log K_a vs 1/T plot observed between $LiAlH_4$ and $NaAlH_4$ parallels that seen in the comparison of the center-to-center distances for the ion pair at 25°C contained in Table 37. The fact that the radius derived from the experimental K_a is approximately midway between the values calculated from the crystal radii and the proposed model further substantiates the presence of both types of ion pairs in THF solutions of $NaAlH_4$.

The change of entropy on dissociation can be calculated from the experimental K_a's and the calculated ΔH_d° values. The entropies of dissociation for the $LiAlH_4$ ion pair are calculated to be -36 and -34 cal/mole-deg at 25° and -70°C, respectively. The corresponding parameters for $NaAlH_4$ at 25° and -70°C are -44 and -25 cal/mole-deg. The large negative values observed are consistent with the ΔS_d° values found by previous workers[25,26] for systems containing solvent separated and contact ion pairs. At -70°C the ΔS_d° has increased by 50% over that at 25°C for $NaAlH_4$, indicating that the dissociation process at -70°C occurs with less change in the orientation of the solvent around the ions.

The association curves for $LiAlH_4$ and $NaAlH_4$ are virtually identical in THF, and are consistent with the presence of ion pairs and triple ion aggregates. A limiting i-value of 1.5 at the higher concentrations is consistent with equal amounts of the two possible triple ions being present in the solution. The conductance data for $LiBH_4$ in THF indicate that $LiBH_4$ is more associated than $LiAlH_4$ even in dilute solution and it is likely that the triple ion is the predominant species since an i-value

of 1.5 is observed over most of the concentration range studied. More extensive association is expected for $LiAlH_4$ and $LiBH_4$ in diethyl ether than in THF because of the much lower dielectric constant (4.34 vs. 7.60) and the reduced solvating power of the oxygen of diethyl ether. Consequently, the higher association values and the conductance data indicate that the ion aggregates in these solutions contain ions in contact.

All of the methoxy derivatives except $LiAl(OCH_3)H_3$ exhibit substantially higher i-values than those found for the parent hydride. This is apparently due to the ability of the oxygen of the methoxy group to coordinate the lithium ion and displace the solvent molecules. When two or more methoxy substituents are present, chain-like structures (I) are possible. The unique shape of the association curves of the di- and tri-

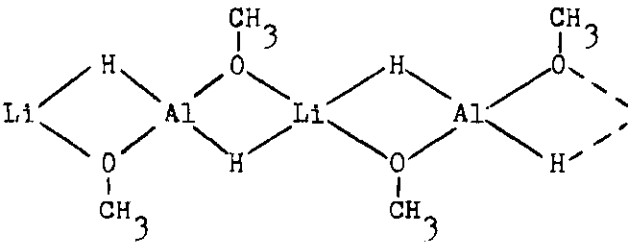

(I)

substituted methoxy derivatives indicate that linear chains joined by a methoxy bridge are occuring. This would account for the insolubility of the tetramethoxy derivatives and the apparent disproportionation of the trimethoxy derivatives.

The replacement of the methoxy substituents with the larger tert-butoxy and diphenylmethylcarbonyloxy substituents apparently inhibits the formation of these chains via steric hindrance. Since the i-values

for all these alkoxy derivatives do not exceed 1.2 even at high concentration, ion pairs are probably the predominant species present in solution.

At the concentration usually employed in reductions with $LiAlH_4$, $NaAlH_4$ and $LiBH_4$ in THF and diethyl ether the fraction present as free ions is very small; consequently, it is reasonable to assume that the ion pair or triple ion is the reducing species. Furthermore, these solute species may be solvent separated, in intimate contact or may be mixtures of solvent separated and contact species.

NMR studies and infrared studies[27] have shown that specific solvation by four molecules of acetone occurs at the lithium ion for lithium iodide and lithium perchlorate in acetone-nitromethane mixtures. Furthermore, conductance data[39] are consistent with the presence of solvent separated ion pairs for these salts in acetone. Specific solvation by four molecules of THF at the lithium ion is also observed for these salts in THF-diethyl ether mixtures and the formation of lithium ion-acetone complex is found both in THF and diethyl ether. Consequently it appears that solvation occurs at the lithium ion in the solvent separated ion pairs by coordination with the oxygen having the greatest solvating power.

Since the $LiAlH_4$ ion pair is a solvent separated ion pair in THF, it is probable that the initial step in the reaction is the complexation by a carbonyl oxygen of the lithium ion followed by a hydride transfer. The specific solvation of the sodium ion is usually less than that found for the lithium ion because of its larger size. Since the conductance data are consistent with the presence of both solvent separated and

contact solute species, initial complexation by the carbonyl oxygen at the sodium ion is less likely to occur. Therefore, it is reasonable to expect that a difference in the selectivity of $NaAlH_4$ and $LiAlH_4$ in THF will occur.

The reaction of 3,3,5-trimethylcyclohexanone with $LiAlH_4$ and $NaAlH_4$ in THF[38] are both concentration dependent; the stereoselectivity, as measured by the formation of the less stable alcohol in the product, increases with decreasing concentration, i.e., from 0.5 M to 0.001 M. Although the selectivity of $LiAlH_4$ and $NaAlH_4$ are comparable at the most dilute concentration studied, the selectivity of $LiAlH_4$ is significantly greater than that found for $NaAlH_4$ at the higher concentrations. Evidently the ion pair is the active reducing species in these solutions, and the solvent separated ion pair appears to give the greatest stereoselectivity.

In order to determine the extent of the stereoselectivity of the solvent separated ion pair, a comparison was made of the stereochemical results obtained from the reduction of several ketones with the parent hydrides in THF.[38] These results are tabulated in Table 38. With three of the ketones studied, the yield of the less stable alcohol found in the product is significantly smaller for $NaAlH_4$ compared to that of $LiAlH_4$. A comparison of the data for $LiBH_4$ with the $LiAlH_4$ data shows that the percentage of the less stable alcohol found in the product is also smaller for $LiBH_4$ with four of the ketones studied. A similar conclusion is reached when the results of $LiBH_4$ are compared to those of $NaAlH_4$. Apparently, the enhanced selectivity of the solvent separated $LiAlH_4$ ion pairs can be attributed to the ability of the lithium ion to complex the

carbonyl oxygen with the displacement of solvent. The decreased selectivity of $LiBH_4$ can be attributed to the decreased availability of the lithium ion to complex the ketone because triple ions are present with the ions in intimate contact. Intermediate results are obtained for $NaAlH_4$ because substantial amounts of contact ion pairs are present and because the sodium ion is a poorer complexing cation than the lithium ion.

In reductions with $LiAl(OCH_3)_3H$, it is reasonable to expect that the active reducing species is also the ion pair. Although larger aggregates are formed at the higher concentrations, the ion pair is present at the dilute concentrations. Furthermore, an equilibrium between the larger aggregates and the ion pair is suggested because the equivalent conductance is constant over a wide concentration range. The similarity in the

$$[LiAl(OCH_3)_3H]_3 \rightleftharpoons [LiAl(OCH_3)_3H]_2 + LiAl(OCH_3)_3H$$

equivalent conductance of $LiAl(OCH_3)_3H$ and 0.10 M $LiAlH_4$ solutions suggest that this is a solvent separated ion pair. Consequently, it would be reasonable to expect an increase in selectivity since the $Al(OCH_3)_3H^-$ ion is sterically larger than the AlH_4^- ion. On the other hand, $LiAl(Ot\text{-}Bu)_3H$ is apparently a contact ion pair, and it is reasonable to expect that the selectivity should be compapable to that found for $LiAlH_4$ for two opposing reasons: (1) Since $LiAl(Ot\text{-}Bu)_3H$ is a contact ion pair, the decreased availability of the lithium ion for complexation should decrease selectivity. (2) Increased selectivity should be observed because the $Al(Ot\text{-}Bu)_3H^-$ ion is larger sterically than the AlH_4^- ion.

Another reaction pathway is indicated by the fact that Bu_4NaAlH_4

in THF reacts with these ketones. It is reasonable to expect that complexation of the carbonyl oxygen by Bu_4N^+ ion would be minimal because of its large size. Furthermore, NMR experiments indicate that there is little specific solvation of this compound by THF. The conductance data are also consistent with the presence of contact ion pairs, and the stereoselective results shown in Table 38 exhibit a decreased selectivity with three of the ketones studied. In the absence of a cation such as lithium, it appears likely that there is direct bimolecular attack of the AlH_4^- ion at the carbonyl group without prior complexation. Consequently, this mode of attack must be considered a possibility for reductions involving the other complex metal hydrides.

Obviously, the ketone plays an important role in selectivity and cannot be entirely discounted. The evaluation of other complex metal hydrides in reactions with various ketones is required before selectivity can be comprehensively explained. These results, however, suggest strongly that initial complexation by the cation with displacement of solvent occurs in these reductions and may provide an explanation for the enhanced selectivity of the solvent separated ion pair.

APPENDIX

Derivation 1. Derivation of the Fuoss Equation Used to Estimate the Ion Pair Dissociation Constant.

Several methods are available for the evaluation of the dissociation constant (K_a) and the equivalent conductance at infinite dilution (Λ_o) of a weak electrolyte[24,31] from conductance measurements. The Fuoss treatment is used in these studies. The derivations are from Fuoss and Accascina.[24]

Definitions

K_a = Ion Pair Dissociation Constant

AB = Ion Pair

α = Degree of Ionization of the Ion Pair

C = Concentration

Λ = Equivalent Conductance

$\gamma_{\pm}$ = Activity Coefficient Ions

Equilibrium

$$AB \rightleftharpoons A^+ + B^-$$

$$K_a = \frac{\alpha^2 C \gamma_{\pm}^2}{(1-\alpha)}$$

The degree of ionization (α) is defined by Fuoss according to the semi-empirical relationship

$$\alpha = \frac{\Lambda}{\Lambda_o (1 - S\sqrt{C\alpha}/\Lambda_o)} = \frac{\Lambda}{\Lambda_o F}$$

where S is the Onsager coefficient. The function F is the continued fraction

$$F = 1 - Z(1 - Z[1 - Z\{1 - . \quad . \quad .\}^{-\frac{1}{2}}]^{-\frac{1}{2}})^{-\frac{1}{2}}$$

or

$$F = \frac{4}{3}\cos^2\left(\frac{1}{3}\cos^{-1}\left[1 - 3\sqrt{3Z}/2\right]\right)$$

where Z is defined as

$$Z = S(\Lambda C)^{\frac{1}{2}}/\Lambda_o^{3/2}$$

The activity coefficient ($\gamma_{\pm}$) is evaluated from the Debye-Hückel limiting law

$$\log \gamma_{\pm} = -\beta\sqrt{\alpha C}$$

where β is a defined constant.

Substitution of the equation for α into the equilibrium expression yields the Fuoss equation.

$$\frac{F}{\Lambda} = \frac{1}{\Lambda_o} + \frac{C\Lambda\gamma_{\pm}^2}{F(\Lambda_o)^2 K_a}$$

An estimate of Λ_o is obtained from a plot of Λ vs. $\sqrt{C}$, from use of the Walden product, or Λ_o from similar salts. Then for each concentration, a Z is calculated and a F is determined. Substitution of the appropriate values into the Fuoss equation, and calculations of F/Λ and $C\Lambda\gamma_{\pm}^2/F$ yields a least squares plot with an intercept of $1/\Lambda_o$ and a slope of $1/K_a(\Lambda_o)^2$. The iterative process is continued until the values of Λ_o and K_a are constant for the data. A computer program to perform these calculations is entitled "FUOSS".

Derivation 2. Derivation of the Fuoss Equation Used to Estimate the Triple Ion Dissociation Constant.

Definitions

α_1 = Fraction Present as Free Ions

α_3 = Fraction Present as Triple Ions

C = Concentration

K_a = Ion Pair Dissociation Constant

K_t, k_1, k_2 = Triple Ion Dissociation Constants

Λ_o = Equivalent Conductance at Infinite Dilution (Ion Pair)

λ_o = Equivalent Conductance at Infinite Dilution (Triple Ion)

A^+, B^- = Free Ions

AB = Ion Pair

ABA^+, BAB^- = Triple Ions

$\gamma_\pm, \gamma_+, \gamma_+^t$ = Activity Coefficients

Equilibria

$$AB \overset{K_a}{\rightleftharpoons} A^+ + B^-$$

$$ABA^+ \overset{k_1}{\rightleftharpoons} AB + A^+$$

$$BAB^- \overset{k_2}{\rightleftharpoons} AB + B^-$$

Assuming $k_1 = k_2 = K_t$, then the corresponding equilibrium constant expressions are

$$K_a = \frac{\alpha_1^2 C \gamma_\pm^2}{(1 - \alpha_1 - 3\alpha_3)}$$

$$K_t = \frac{(1 - \alpha_1 - 3\alpha_3)\alpha_1 C \gamma_\pm}{\alpha_3 \gamma_+^t}$$

If all activity coefficients and the quantity $(1 - \alpha_1 - 3\alpha_3)$ are all set equal to one, the simplified equations become respectively

$$K_a = \alpha_1^2 C$$

$$K_t = \frac{\alpha_1 C}{\alpha_3}$$

Therefore,

$$\alpha_1 = \sqrt{K_a/C}$$

and

$$\alpha_3 = \sqrt{CK_a}/K_t$$

Assuming ion pairs and triple ions to be present in solution, the conductance equation is

$$\Lambda = \alpha_1 \Lambda_o + \alpha_3 \lambda_o$$

Substituting

$$\Lambda = (\sqrt{K_a}/C)(\Lambda_o) + (\sqrt{K_a C}/K_t)(\lambda_o)$$

The above equation is of the form,

$$\Lambda = A C^{-\frac{1}{2}} + B C^{\frac{1}{2}}$$

If the concentration of solute is very dilute, the concentration of triple ion is not important and the $BC^{\frac{1}{2}}$ term is small. Hence,

$\Lambda \approx AC^{-\frac{1}{2}}$ and a plot of log Λ versus log C should approach linearity with a slope equal to 0.5 at low concentrations in solvents of low dielectric constant. This equation is used as a test for the absence of triple ion on data where the ion pair dissociation constant is evaluated. For the evaluation of the triple ion dissociation constant K_t, however, the equation is put into a more convenient form by multiplication by $C^{\frac{1}{2}}$.

$$\Lambda C^{\frac{1}{2}} = A + BC$$

At this time mobility and Arrhenius correction terms[24] (g(C)) are introduced giving the experimentally usable form of the equation.

$$\Lambda C^{\frac{1}{2}}\, g(C) = \Lambda_o\, K_a^{\frac{1}{2}}(\lambda_o K_a^{\frac{1}{2}}/K_t)\,(1 - \Lambda/\Lambda_o)C$$

A plot of $\Lambda C^{\frac{1}{2}} g(C)$ versus $(1 - \Lambda/\Lambda_o)C$ is linear, and the triple ion dissociation constant K_t can be estimated from the slope of the line, since K_a is known and λ_o is assumed to $\Lambda_o/3$. A least squares computer program to perform these calculations is entitled "K3TRIP".

Derivation 3. The Calculation of the Concentration of Species Present in Solution Assuming Only Ion Pairs and Triple Ions.

Definitions

Same as in Derivation 2.

Equilibria

Same as in Derivation 2.

The appropriate equilibrium constant expressions are:

$$K_a = \frac{\alpha_1^2 C \gamma_\pm^2}{(1 - \alpha_1 - 3\alpha_3)}$$

$$K_t = \frac{(1 - \alpha_1 - 3\alpha_3) C \gamma_+}{\alpha_3 \gamma_+^t}$$

The total concentration M is equal to the concentration of ion pair, free ions and triple ions, i. e.,

$$M = (1 - \alpha_1 - 3\alpha_3)C + \alpha_1 C + 3\alpha_3 C$$

The activity coefficients for the respective ions are obtained from the extended form of the Debye-Hückel law where a_1 and a_3 are the center-to-center distances between the ions in the ion pair and triple ion, respectively.

$$\log \gamma_\pm = \frac{-A I^{\frac{1}{2}}}{1 + Ba_1 I^{\frac{1}{2}}}$$

$$\log \gamma_{+} = \frac{-A\, I^{\frac{1}{2}}}{1 + Ba_1 I^{\frac{1}{2}}}$$

$$\log \gamma_{+}^{t} = \frac{-A\, I^{\frac{1}{2}}}{1 + Ba_3 I^{\frac{1}{2}}}$$

Both A and B can be evaluated. The ionic strength is defined

$$I = 1/2(\alpha_1 C + \alpha_1 C + \alpha_3 C + \alpha_3 C) = \alpha_1 C + \alpha_3 C$$

Using an iterative procedure, values for α_1 and α_3 are determined until no change occurs in these values. Then the concentration of ion pairs, free ions and triple ions can be calculated. A computer program designed to perform these calculations is entitled "COMP3".

COMPUTER PROGRAMS

The RCA Spectra-70 Computer at Georgia State University was used exclusively to perform all calculations. The computer programs were written in the BASIC Language. The following programs were used:

1. FUØSS - This program was designed to calculate the Λ_o and K_a values from conductance data in the most dilute concentration range.
2. KJTRIP - This program was designed to calculate the triple ion dissociation constant (K_t) in the region of the minimum from conductance data.
3. CØMP3 - This program was designed to calculate the fraction of ions, ion pairs and triple ions at any concentration using the K_a and K_t values obtained from conductance data.
4. DELTAT - This program was designed to calculate the association i-values from the ebullioscopic data.
5. AVALUE - This program was designed to calculate the center-to-center distance between the ions in the ion pair from the experimental K_a value.

FUØSS

```
4 PRINT " THE VALUES OF K, A1, T, N  ARE ????"
5 INPUT K, A1, T, N
10 DIM C(50), L(50), A(50), Z(50), F(50), Y(50), G(50), X(50)
11 DIM  D(50), H(50)
23 PRINT "  K","    A1","    T","    N"
25 PRINT K, A1, T, N
27 FØR L=1  TØ 7
31 PRINT
34 FØR I=1  TØ N
35 READ C(I), L(I)
40 LET A(I)=K*L(I)*1.0E3/C(I)
45 LET D= -1.49 + 2660/T
47 LET V=10.0↑ (-3.655 + 393/T)
50 LET S=(8.183E5*A1)/( (D*T)↑1.5) +82.00/(V*SQR(D*T))
60 LET B=1.815E6/(D*T)↑1.5
70 LET Z(I)=(S*SQR(A(I)*C(I)))/(A1)↑1.5
75 LET F(I)=1.0-Z(I)*(1.0-z(I)*(1.0-Z(I))↑.5)↑.5
80 LET Y(I)=F(I)/A(I)
90 LET G(I)=10.0↑(-B*SQR(C(I)*A(I)/(A1*F(I))))
95 LET D(I)=A(I)/(A1*F(I))
100 LET X(I)=C(I)*(G(I)↑2)*A(I)/F(I)
104 LET H(I)=SQR(C(I))
105 NEXT  I
106 PRINT
107 PRINT
108 RESTORE
120 LET X=0
125 LET Y=0
130 LET M=0
135 LET X2=0
140 FØR I=1 TØ N
145 LET X=X+X(I)
150 LET Y=Y+Y(I)
155 LET M=M+X(I)*Y(I)
160 LET X2=X2+X(I)↑2
165 NEXT I
170 LET Y(A)=Y/N
175 LET X(A)=X/N
180 LET S1=M-X*Y/N
185 LET S2=X2-X↑2/N
190 LET B1=S1/S2
195 LET B0=Y(A)-B1*X(A)
200 LET A1=1/B0
205 LET K(L)=1/(B1*A1 2)
207 PRINT L
208 PRINT "CALC A1","SLOPE,B1","INTERCEPT,B0", EQUI CØNSTANT,K(L)"
209 PRINT
210 PRINT A1,B1,B0,K(L)
211 PRINT
215 NEXT L
```

FUØSS

```
225 PRINT "    C(I)","     A(I)","     D(I)"
230 FØR I=1   TØ N
231 PRINT C(I),A(I),D(I)
232 NEXT I
233 PRINT
234 PRINT
235 PRINT "    X(I)","    Y(I)","    SQR  C(I)"
240 FØR I=1 TØ N
242 PRINT X(I),Y(I),H(I)
245 NEXT I
300 DATA STATEMENTS
320 END
```

K3TRIP

```
  5 PRINT "VALUES ØF K,A1,T,N,K1 ARE ?"
  6 INPUT K,A1,T,N,K1
 10 DIM C(30),L(30),A(30),G(30),X(30),Y(30)
 11 DIM H(30),E(30)
 30 FØR I=1 TØ N
 35 READ C(I),L(I)
 37 LET D=-1.49+2.66E3/T
 39 LET V=10.0↑(-3.665+393/T)
 40 LET A(I)-K*L(I)*1.0E3/C(I)
 50 LET S=(8.183E5*A1)/((D*T)↑1.5)+82.00/(V*SQR(D*T))
 60 LET B=1.815E6/(D*T)↑1.5
 65 LET H(I)=(1.0-S*SQR(C(I)*A(I)/A1 3)))
 70 LET G(I)=10.0↑(B*SQR(C(I)*A(I)/A1))/(H(I)*SQR(1.0-A(I)/A1))
 80 LET Y(I)=A(I)*SQR(C(I))*G(I)
 90 LET X(I)=(1.0-A(I)/A1)*C(I)
 95 LET E(I)=A(I)*SQR(C(I))
105 NEXT I
106 PRINT
107 PRINT
120 LET X=0
125 LET Y=0
130 LET M=0
135 LET X2=0
140 FØR I=1 TØ N
145 LET X=X+X(I)
150 LET Y=Y+Y(I)
155 LET M=M+X(I)*Y(I)
160 LET X2=X2+X(I)↑2
165 NEXT I
170 LET Y(A)=Y/N
175 LET X(A)=X/N
180 LET S1=M-X*Y/N
185 LET S2=X2-X↑2/N
190 LET B1=S1/S2
195 LET BO=Y(A)-B1*X(A)
200 LET K2=(BO/A1)↑2
205 LET K3=(A1*SQR(K1))/(3.0*B1)
208 PRINT "   Y(I)","   X(I)","   A(I)","   C(I)","   A*SQR C"
210 FØR I=1 TØ N
220 PRINT Y(I),X(I),A(I),C(I),E(I)
221 NEXT I
222 PRINT
225 PRINT
226 PRINT "   SLOPE, B1","    INTERCEPT,BO"
227 PRINT B1,BO
230 PRINT
231 PRINT
232 PRINT
235 PRINT "THE IØN PAIR CØNST.,K1";K1
```

K3TRIP (Continued)

```
237 PRINT
240 PRINT "THE TØN PATR CØNST. CALCD FROM TRIPLE IØN DATA, K2";K2
242 PRINT
245 PRINT "THE TRIPLE TØN DISS. CØNST., K3 IS';K3
247 PRINT
250 PRINT
251 PRINT "D IS";D,"    V IS";V
300 DATA STATEMENTS
350 END
```

COMP3

```
2  PRINT "THE VALUES OF K1,K3,T?"
10 INPUT K1,K3,T
20 LET G=1
30 LET Q=100
40 LET G2=1
45 LET C=1E-8
50 LET D1=-1.49+2.66E3/T
60 LET B1=1.290E6/(D1*T)↑1.5
70 LET A1=35.56*5/(D1*T)↑1.5
80 LET A3=35.56*10/(D1*T)↑1.5
100 LET S=(-K1+SQR(K1↑2+(4*C*K1*G↑2)))/(2*C*G↑2)
110 LET S3=S*C*G*(1-S)/(K3*G2+3*S*C*G)
120 LET S1=(-K1+SQR(K1↑2-(4*C*K1*G↑2*(3*S3-1))))/(2*C*G↑2)
130 LET S4=S1*C*G*(1-S1)/(K3*G2+3*S1*C*G)
135 LET S2=(-K1+SQR(K1↑2-(4*C*K1*G↑2*(3*S4-1))))/(2*C*G↑2)
140 LET I=(S2+S4)*C
150 LET G=10.0↑(-B1*SQR(I)/(1+A1*SQR(I)))
160 LET G2=10.0↑(-B1*SQR(I)/(1+A3(SQR(I)))
170 LET G3=G/G2
315 LET S5=S2*C*G*(1-S2)/(K3*G2+3*S2*C*G)
320 LET S7=(-K1+SQR(K1↑2-(4*C*K1*G  2*(3*S4-1))))/(2*C*G↑2)
330 LET S8=S7*C*G*(1-S7)/K3*G2+3*S7*C*G)
335 LET S9=(-K1+SQR(K1↑2-(4*C*K1*G↑2*(3*S8-1))))/(2*C*G↑2)
340 LET I1=(S9+S8)*C
342 LET G=10.0↑(-B1*SQR(I1)/(1+A1*SQR(I1)))
344 LET G2=10.0↑(-B1*SQR(I1)/(1_A3*SQR(I1)))
350 LET Q=S9*C*G*(1-S9)/(K3*G2+3*S9*C*G)
355 LET QL=(-K1+SQR(K1↑2-(4*C*K1*G↑2*(3*Q-1))))/(2*C*G↑2)
360 LET Q2=Q1*C*G*(1-Q1)/(K3*G2+3*Q1*C*G)
362 LET Q3=(-K1+SQR(K1↑2-(4*C*K1*G↑2*(3*Q2-1))))/(2*C*G↑2)
374 PRINT S,S1
375 PRINT S2,S7,S9,Q1,Q3
376 PRINT S3,S4,S5,S8,Q
377 PRINT Q2
379 PRINT "CONC.", "F ION PRS.","F TRIPLES","ACT. IP","ACT.T"
380 PRINT C,Q3,Q2,G,G2
381 PRINT
382 LET C=10*C
385 IF C>=2 THEN 400
395 GO TO 50
400 END
```

DELTAT

```
1 DIM X(30),Y(30),M(30),R(30),P(30),K(30)
2 DIM T(30),A(30),C(30),W(30),V(30)
10 PRINT "THE VALUES ØF M,H,N, ARE?"
15 INPUT M,H,N
18 PRINT
19 PRINT "K1","K2","K3","K4","K5"
20 FØR I=1 TØ N
30 READ T(I),W(I),V(I)
35 LET X(I)=1.0-2.71828↑(-T(I)*M/2200)
40 LET M(I)=W(I)/H
45 LET R(I)=V(I)/M
50 LET P(I)=M(I)+R(I)
55 LET Y(I)=M(I)/P(I)
70 LET K1=(Y(I)-X(I))/(X(I)↑2)
75 LET K2=(Y(I)-X(I))/((2*X(I)-Y(I))↑2)
80 LET K3=((Y(I)-X(I))*4)/((3*X(I)-Y(I))↑3)
85 LET K4=((Y(I)-X(I))*27)/((4*X(I)-Y(I))↑4)
90 LET K5=((Y(I)-X(I))*256)/((5*X(I)-Y(I))↑5)
95 LET K(I)=((Y(I)-X(I))*3125)/((6*X(I)-Y(I))↑6)
97 LET A(I)=((W(I)*M)/(V(I)*H))*(1.0/X(I))
98 LET C(I)=M(I)*1000/W(I)
99 PRINT K1,K2,K3,K4,K5
100 NEXT I
105 PRINT
134 PRINT
135 PRINT
136 PRINT "K6","XS","XE","I VALUE","CØNC."
140 FØR I-1 TØ N
145 PRINT K(I),Y(I),X(I),A(I),C(I)
150 NEXT I
300 DATA STATEMENTS
350 END
```

AVALUE

```
2 DIM A(50),B(50),Y(50),K(50),X(50)
4 PRINT "THE VALUE ØF T?"
5 INPUT T
9 FØR I=1 TØ 45
10 READ A(I)
30 LET D=-1.49+2660/T
35 LET B(I)=(4.803E-10↑2)/(A(I)*D*1.380E-16*T)
40 LET Y(I)=4*3.1416*6.022E23*(A(I)↑3))
42 LET X(I)=(3000)/Y(I)
45 LET K(I)=(X(I))*(2.71828↑(-B(I)))
50 NEXT I
52 PRINT "K(I)","A VALUE,CM"
55 FØR I=1 TØ 45
59 PRINT
60 PRINT K(I),A(I)
65 NEXT I
100 DATA STATEMENTS
150 END
```

Table 1. Elemental Analysis for the Alkoxy Derivatives of $LiAlH_4$.

Compound	Sample Weight, mg	Active Hydride, mmole	Aluminum mmole	H/Al
$LiAlH_4$	350.0	2.44	0.606	4.02
$LiAl(OCH_3)H$	559.2	3.20	1.08	3.09
$LiAl(OCH_3)_2H_2$	485.4	0.674	0.737	1.88
$LiAl(OCH_3)_3H$	506.0	0.670	0.642	1.01
$LiAl(OCH_3)_4$	80.1	0.926	3.16	0.29
$LiAl(O\text{-}tBu)H_3$	609.2	2.38	0.793	3.01
$LiAl(O\text{-}tBu)_3H$	550.0	0.640	0.608	1.05
$LiAl(OCHPh_2)H$	792.6	2.90	0.963	3.02
$LiAl(OCHPh_2)_3H$	2257.8	1.96	2.05	0.96

Table 2. Elemental Analyses for the Alkoxy Derivatives of $LiBH_4$.

Compound	Sample Weight, mg	Active Hydride, mmole	Lithium mmole	H/Li
$LiBH_4$	323.0	1.86	0.463	4.04
$LiB(OCH_3)H_3$	486.0	2.07	0.668	3.10
$LiB(OCH_3)_2H_2$	778.6	1.02	0.405	2.54
$LiB(OCH_3)_3H$	980.3	0.630	0.651	0.97
$LiB(OCH_3)_4$	163.5	0.778	5.91	0.13
$LiB(O\text{-}tBu)H_3$	452.9	1.50	0.482	3.11
$LiB(O\text{-}tBu)_3H$	711.1	0.825	0.639	1.26
$LiB(OCHPh_2)H_3$	857.4	1.67	0.536	3.11
$LiB(OCHPh_2)_3H$	1052.9	0.516	0.537	0.96

Table 3. Equivalent Conductance of $LiAlH_4$ in Tetrahydrofuran at 25°C

Conc., $\underline{M}(10^6)$	$\Lambda(\frac{mhos}{cm^2})$	Conc., $\underline{M}(10^6)$	$\Lambda(\frac{mhos}{cm^2})$
0.157	71.1	416	3.94
0.320	57.5	5.93	29.6
1.20	44.2	41.1	10.6
4.16	31.3	45.5	10.2
6.05	24.9	50.1	9.81
9.96	23.0	55.7	9.16
12.1	20.3	62.2	8.67
16.4	16.0	70.0	8.25
34.8	12.6	81.3	7.58
66.2	9.09	93.6	7.19
71.0	8.93	108	6.59
81.7	8.37	128	6.11
93.0	7.86	175	5.66
112	7.27	193	5.46
135	6.91	219	5.09
169	6.01	247	4.71
193	5.69	288	4.37
225	5.27	340	4.01
257	4.97	426	3.58
300	4.63		
346	4.31		

Table 3. Equivalent Conductance of $LiAlH_4$ in THF at 25°C from 5×10^{-4} M to 0.1 M. (Continued)

Conc., M	$\Lambda(\frac{mhos}{cm^2})$	Conc., M	$\Lambda(\frac{mhos}{cm^2})$
4.90×10^{-4}	3.68	6.33×10^{-3}	1.51
7.11×10^{-4}	3.54	8.14×10^{-3}	1.43
7.91×10^{-4}	3.37	1.14×10^{-2}	1.26
8.90×10^{-4}	3.22	2.29×10^{-2}	1.27
1.02×10^{-3}	3.03	2.63×10^{-2}	1.29
1.19×10^{-3}	2.82	3.05×10^{-2}	1.35
1.42×10^{-3}	2.63	3.38×10^{-2}	1.36
1.78×10^{-3}	2.39	3.97×10^{-2}	1.42
2.11×10^{-3}	2.22	5.07×10^{-2}	1.57
2.49×10^{-3}	2.07	6.08×10^{-2}	1.86
3.00×10^{-3}	1.94	7.03×10^{-2}	1.90
3.56×10^{-3}	1.82	7.95×10^{-2}	2.07
4.38×10^{-3}	1.69	9.14×10^{-2}	2.30
5.18×10^{-3}	1.59	1.01×10^{-1}	2.51

Table 4. Equivalent Conductance of $LiAlH_4$ in THF at 25°C from 0.06 M to 1.5 M. (Cell Constant = 1.123 cm^{-1})

Conc., M	Λ ($\frac{mhos}{cm^2}$)	Conc., M	Λ ($\frac{mhos}{cm^2}$)
0.058	1.34	0.278	5.26
0.073	1.55	0.308	5.81
0.087	1.65	0.399	7.23
0.101	1.92	0.478	8.69
0.114	2.20	0.546	9.70
0.140	2.73	0.695	11.00
0.165	3.19	0.790	11.48
0.189	3.76	0.900	11.20
0.212	4.19	1.080	9.30
0.246	4.80	1.540	6.43

Table 5. Equivalent Conductance of $NaAlH_4$ in Tetrahydrofuran at 25° C.

Conc., $\underline{M}(10^6)$	$\Lambda(\frac{mhos}{cm^2})$	Conc., $\underline{M}(10^6)$	$\Lambda(\frac{mhos}{cm^2})$
0.174	64.4	78.9	4.13
0.523	49.5	80.9	4.03
2.14	21.3	133	3.41
3.70	19.7	139	3.29
5.76	13.0	156	3.13
10.0	12.5	211	2.69
17.9	8.72	227	2.58
25.0	8.31	290	2.35
30.2	7.69	383	1.98
31.9	7.03	550	1.71
43.5	5.81		

Table 5. Equivalent Conductance of $NaAlH_4$ in Tetrahydrofuran at 25°C from 0.001 M to 0.5 M. (Continued)

Conc., M	Λ ($\frac{mhos}{cm^2}$)	Conc., M	Λ ($\frac{mhos}{cm^2}$)
1.15×10^{-3}	1.191	3.64×10^{-2}	0.608
2.49×10^{-3}	0.854	4.31×10^{-2}	0.642
3.95×10^{-3}	0.679	5.26×10^{-2}	0.695
7.39×10^{-3}	0.445	6.11×10^{-2}	0.740
9.82×10^{-3}	0.409	7.29×10^{-2}	0.821
1.22×10^{-2}	0.440	8.61×10^{-2}	0.903
1.46×10^{-2}	0.461	1.05×10^{-1}	1.04
1.69×10^{-2}	0.471	1.35×10^{-1}	1.31
1.92×10^{-2}	0.483	1.58×10^{-1}	1.57
2.15×10^{-2}	0.492	1.89×10^{-1}	1.98
2.48×10^{-2}	0.522	2.37×10^{-1}	2.59
2.53×10^{-2}	0.543	3.16×10^{-1}	3.64
2.79×10^{-2}	0.573	4.02×10^{-1}	5.50
3.16×10^{-2}	0.586	4.96×10^{-1}	8.05

Table 6. Equivalent Conductance of $LiBH_4$ in Tetrahydrofuran at 25° C.

Conc., M (10^6)	$\Lambda(\frac{mhos}{cm^2})$	Conc., M(10^4)	$\Lambda(\frac{mhos}{cm^2})$
0.25	4.98	7.50	0.082
1.00	2.49	8.39	0.069
2.06	1.66	8.95	0.053
2.25	1.49	9.18	0.039
2.77	1.39	10.1	0.038
4.09	1.24	15.1	0.034
9.14	0.83	24.8	0.029
20.7	0.55	39.3	0.026
50.4	0.36	58.2	0.023
77.8	0.29	80.1	0.022
143	0.21	192	0.016
222	0.16	287	0.017
420	0.12	546	0.019
648	0.10	658	0.024
		762	0.027
		998	0.029

Table 7. Equivalent Conductance of $LiBH_4$ in Tetrahydrofuran at 25°C from 0.03 M to 1.0 M. (Cell Constant = 1.123 cm^{-1}).

Conc., M	Λ ($\frac{mhos}{cm^2}$)	Conc., M	Λ ($\frac{mhos}{cm^2}$)
0.036	0.0095	0.565	0.260
0.105	0.0286	0.683	0.359
0.191	0.0567	0.781	0.454
0.265	0.108	0.870	0.521
0.353	0.127	0.981	0.594
0.463	0.191	1.062	0.548

Table 8. Equivalent Conductance of Bu_4NAlH_4 in THF at 25° C.

Conc., M (10^6)	Λ ($\frac{mhos}{cm^2}$)	Conc., M (10^4)	Λ ($\frac{mhos}{cm^2}$)
0.13	81.1	7.5	5.49
0.52	66.3	8.75	5.11
1.97	59.4	10.0	4.75
5.06	43.6	25.0	4.29
11.1	32.5	50.0	4.00
25.0	25.5	62.5	3.83
56.3	17.5	75.0	3.70
121.1	12.2	87.0	3.60
260	8.65	100	3.50
634	5.92	235	3.30

Table 9. Limiting Conductances and Equilibrium Constants of Dissociation of the Complex Metal Hydrides in THF at 25° C.

Compound	$\Lambda_o \left(\frac{\text{mhos}}{\text{cm}^2}\right)$	K_a	K_t*
$LiAlH_4$	90	0.69×10^{-6}	1.8×10^{-3}
$NaAlH_4$	81	0.21×10^{-6}	3.8×10^{-3}
Bu_4NAlH_4	97	0.18×10^{-5}	1.4×10^{-3}
$LiBH_4$**	80	1.0×10^{-9}	8.2×10^{-3}

*The Fuoss treatment employed for the determination of K_t from the conductance data assumes that the formation constants for the two types of triple ions are equal.

**Since the conductance of the $LiBH_4$ solutions are low even at 10^{-7} M, the values obtained for this hydride are not as reliable as the other K_a's in the Table.

Table 10. Equivalent Conductance of $LiAlH_4$ in Tetrahydrofuran at Several Temperatures (Experiment 1).

	Concentration, $\underline{M}(10^5)$				
Temp., °C	4.85	6.06	58.2	74.9	87.3
25	11.36	10.75	3.87	3.44	3.18
0	12.64	11.78	4.51	3.98	3.70
-15	12.56	11.86	4.51	4.00	3.73
-35	12.09	11.46	4.48	3.95	3.68
-50	11.50	10.99	4.36	3.88	3.62
-70	10.71	10.28	4.16	3.73	3.51

Table 11. Equivalent Conductance of $LiAlH_4$ in Tetrahydrofuran at Several Temperatures (Experiment 2).

	Concentration, $\underline{M}(10^5)$					
Temp., °C	5.54	6.92	24.7	48.0	58.3	72.5
25	9.86	9.44	4.34	3.43	3.29	3.11
10	10.38	9.85	4.65	3.59	3.50	3.34
0	10.98	10.38	5.04	3.81	3.78	3.66
-10	11.31	10.60	5.24	3.91	3.93	3.84
-20	11.55	10.77	5.39	3.99	4.06	3.98
-30	11.59	10.80	5.51	4.03	4.16	4.07
-40	11.46	10.69	5.59	4.03	4.22	4.12
-60	10.29	9.76	5.31	3.83	4.14	4.03
-70	8.90	8.56	4.92	3.55	3.98	3.88

Table 12. Equivalent Conductance of $NaAlH_4$ in Tetrahydrofuran at Several Temperatures.

	Concentration, M (10^5)						
Temp., ° C	2.50	7.89	13.9	19.6	26.9	36.5	84.6
25	8.24	4.12	3.07	2.57	2.31	2.03	1.42
10	8.28	4.47	3.34	2.87	2.57	2.26	1.55
0	8.05	4.71	3.52	3.08	2.75	2.40	1.64
-15	8.01	5.00	3.79	3.70	3.01	2.62	1.76
-20	7.97	5.15	3.89	3.49	3.09	2.70	1.81
-30	7.86	5.34	4.07	3.70	3.28	2.84	1.89
-35	7.78	5.46	4.17	3.80	3.35	2.91	2.05
-40	7.74	5.59	4.26	3.91	3.45	2.99	2.09
-45	7.74	5.69	4.35	4.01	3.51	3.06	2.13
-50	7.66	5.80	4.44	4.11	3.63	3.13	2.18
-60	7.66	6.05	4.63	4.32	3.28	2.26	3.80
-70	7.66	6.24	4.83	4.52	3.97	3.43	2.35

Table 13. Equivalent Conductance of $LiAl(OCH_3)_3H$ in Tetrahydrofuran at 25° C.

Conc., M	Λ ($\frac{mhos}{cm^2}$)	Conc., M	Λ ($\frac{mhos}{cm^2}$)
0.0001	2.21	0.0821	2.42
0.0004	2.22	0.0985	2.32
0.0032	2.21	0.123	2.32
0.0197	2.23	0.164	2.31
0.0246	2.25	0.197	2.31
0.0281	2.23	0.246	2.31
0.0318	2.25	0.328	2.54
0.0365	2.23	0.493	2.70
0.0428	2.32		
0.0518	2.38		
0.0657	2.42		

Table 14. Equivalent Conductance of $LiAl(O\text{-}tBu)_3H$ in Tetrahydrofuran at 25°C.

Conc., M	Λ ($\frac{mhos}{cm^2}$)	Conc., M	Λ ($\frac{mhos}{cm^2}$)
0.0003	0.0095	0.0675	0.0118
0.0020	0.0098	0.0992	0.0124
0.0203	0.0099	0.127	0.0132
0.026	0.0102	0.184	0.0154
0.0289	0.0111	0.225	0.0171
0.0326	0.0112	0.289	0.0208
0.0375	0.0113	0.405	0.0290
0.0440	0.0114		
0.0533	0.0117		

Table 15. Equivalent Conductance of $LiAlH_4$ in Diethyl Ether at 25° C.

Conc., M	Λ ($\frac{\text{mhos}}{\text{cm}^2}$)	Conc., M	Λ ($\frac{\text{mhos}}{\text{cm}^2}$)
0.021	0.0005	0.168	0.0027
0.040	0.0009	0.203	0.0027
0.082	0.0031	0.220	0.0032
0.102	0.0030	0.260	0.0037
0.123	0.0029	0.280	0.0035
0.154	0.0027	0.482	0.0042

Table 16. Association of $LiAlH_4$ in Tetrahydrofuran.

T, ° C	Solute, g	Solvent, g	Concn., m	Association, i
0.098	0.078	45.10	0.043	1.02
0.158	0.138	46.02	0.079	1.10
0.195	0.177	46.52	0.100	1.13
0.257	0.255	47.55	0.141	1.21
0.290	0.314	48.33	0.171	1.29
0.345	0.430	49.86	0.227	1.44
0.367	0.472	50.41	0.241	1.49
0.474	0.689	53.27	0.341	1.57
0.653	1.138	59.18	0.506	1.72
0.807	1.615	65.46	0.650	1.79
1.012	2.353	75.16	0.825	1.82
1.067	2.540	76.68	0.873	1.83

Table 17. Association of $LiAl(OCH_3)H_3$ in Tetrahydrofuran.

T, ° C	Solute, g	Solvent, g	Concn., m	Association, i
0.186	0.216	37.682	0.085	1.00
0.266	0.382	38.788	0.145	1.19
0.354	0.598	40.225	0.219	1.37
0.508	1.124	43.734	0.378	1.65
0.676	1.751	47.917	0.538	1.77

Table 18. Association of $LiAl(OCH_3)_2H_2$ in Tetrahydrofuran.

T, ° C	Solute, g	Solvent, g	Concn., m	Association, i
0.061	0.187	37.443	0.051	1.83
0.113	0.409	39.591	0.105	2.06
0.184	0.786	43.235	0.185	2.22
0.250	1.263	47.850	0.269	2.37
0.321	2.165	56.578	0.390	2.69

Table 19. Association of $LiAl(OCH_3)_3H$ in Tetrahydrofuran

T, ° C	Solute, g	Solvent, g	Concn., m	Association, i
0.009	0.019	34.521	0.004	1.03
0.049	0.159	34.997	0.035	1.56
0.096	0.382	35.755	0.082	1.86
0.125	0.544	36.627	0.113	1.99
0.190	1.034	38.292	0.206	2.38
0.289	1.873	41.139	0.348	2.66
0.375	2.878	44.554	0.493	2.90

Table 20. Association of $LiAl(O\text{-}tBu)H_3$ in Tetrahydrofuran

T, ° C	Solute, g	Solvent, g	Concn., m	Association, i
0.032	0.064	38.653	0.015	1.04
0.104	0.236	39.693	0.054	1.16
0.239	0.589	41.822	0.129	1.19
0.413	1.180	45.394	0.238	1.28
0.692	2.440	53.010	0.422	1.36
0.924	3.745	60.892	0.564	1.36

Table 21. Association of $LiAl(O\text{-}tBu)_3H$ in Tetrahydrofuran

T,° C	Solute, g	Solvent, g	Concn., m	Association, i
0.128	0.559	38.435	0.057	0.98
0.245	1.156	40.581	0.112	1.00
0.448	2.339	44.838	0.205	1.01
0.641	3.668	49.615	0.291	1.00
1.028	7.037	61.728	0.448	0.98
1.343	10.815	75.313	0.565	0.95

Table 22. Association of $LiAl(OCHPh_2)H_3$ in Tetrahydrofuran

T, ° C	Solute, g	Solvent, g	Concn., m	Association, i
0.114	0.438	35.751	0.056	1.07
0.185	0.759	36.531	0.094	1.12
0.240	0.993	37.099	0.122	1.11
0.334	1.627	38.639	0.191	1.26
0.445	2.380	40.469	0.267	1.33
0.625	3.565	43.350	0.374	1.33
0.875	5.453	47.939	0.517	1.32

Table 23. Association of $LiAl(OCHPh_2)_3H$ in Tetrahydrofuran

T, ° C	Solute, g	Solvent, g	Concn., m	Association, i
0.253	2.580	38.040	0.116	1.00
0.515	5.750	40.812	0.241	1.02
0.735	8.389	42.952	0.334	0.99
1.203	13.195	47.155	0.479	0.96

Table 24. Association of $LiBH_4$ in Tetrahydrofuran

T,° C	Solute, g	Solvent, g	Concn., m	Association, i
0.049	0.027	38.664	0.032	1.45
0.172	0.084	40.430	0.091	1.51
0.242	0.164	42.909	0.175	1.59
0.401	0.309	47.411	0.299	1.63
0.602	0.519	53.925	0.441	1.60
1.020	1.130	72.905	0.711	1.56

Table 25. Association of $LiB(OCH_3)H_3$ in Tetrahydrofuran

T,° C	Solute, g	Solvent, g	Concn., m	Association, i
0.057	0.069	38.124	0.035	1.35
0.128	0.203	39.871	0.098	1.69
0.208	0.387	42.265	0.177	1.86
0.321	0.711	46.483	0.295	2.03
0.469	1.152	52.233	0.426	2.01
0.720	2.268	66.769	0.656	2.03

Table 26. Association of $LiB(OCH_3)_2H_2$ in Tetrahydrofuran

T,° C	Solute, g	Solvent, g	Concn., m	Association, i
0.069	0.111	43.818	0.031	0.99
0.111	0.215	49.032	0.053	1.06
0.141	0.405	58.633	0.084	1.32
0.173	0.728	74.871	0.119	1.51
0.288	2.270	94.500	0.294	2.44

Table 27. Association of $LiB(OCH_3)_3H$ in Tetrahydrofuran

T,° C	Solute, g	Solvent, g	Concn., m	Association, i
0.069	0.302	38.524	0.064	2.06
0.130	0.716	43.444	0.135	2.29
0.181	1.325	50.675	0.215	2.61
0.216	2.103	59.924	0.288	2.94
0.252	3.146	72.321	0.357	3.12

Table 28. Association of $LiB(O\text{-}tBu)H_3$ in Tetrahydrofuran

T,° C	Solute, g	Solvent, g	Concn., m	Association, i
0.075	0.103	35.940	0.030	0.90
0.230	0.320	37.517	0.091	0.87
0.385	0.628	39.745	0.168	0.97
0.648	1.218	44.021	0.295	1.01
1.008	2.314	51.964	0.474	1.05

Table 29. Association of $LiB(O\text{-}tBu)_3H$ in Tetrahydrofuran

T,° C	Solute, g	Solvent, g	Concn., m	Association, i
0.182	0.534	36.636	0.061	0.74
0.327	1.081	39.170	0.116	0.79
0.558	2.060	43.529	0.199	0.79
0.865	4.020	52.456	0.322	0.83
1.193	7.320	66.763	0.461	0.87

Table 30. Association of $LiB(OCHPh_2)H_3$ in Tetrahydrofuran

T,° C	Solute, g	Solvent, g	Concn., m	Association, i
0.133	0.476	40.192	0.058	0.96
0.254	0.979	43.633	0.110	0.96
0.350	1.553	47.549	0.160	1.01
0.466	2.366	53.105	0.218	1.02
0.758	5.128	7.972	0.349	1.03

Table 31. Association of $LiB(OCHPh_2)_3H$ in Tetrahydrofuran

T,° C	Solute, g	Solvent, g	Concn., m	Association, i
0.176	1.738	44.023	0.070	0.87
0.290	3.414	48.127	0.125	0.95
0.469	6.178	54.897	0.198	0.94
0.869	14.704	75.781	0.341	0.88

Table 32. Association of $NaAlH_4$ in Tetrahydrofuran

T,° C	Solute, g	Solvent, g	Concn., m	Association, i
0.086	0.073	35.520	0.038	1.00
0.179	0.176	37.155	0.088	1.08
0.257	0.315	39.396	0.147	1.27
0.352	0.558	43.281	0.239	1.50
0.536	1.105	52.079	0.392	1.63

Table 33. Association of $LiAlH_4$ in Diethyl Ether

T,° C	Solute, g	Solvent, g	Concn., m	Association, i
0.110	0.106	31.902	0.087	1.75
0.231	0.254	33.757	0.199	1.90
0.332	0.404	35.625	0.299	1.99
0.472	0.688	39.158	0.463	2.18
0.621	1.163	45.077	0.680	2.43

Table 34. Association of $LiBH_4$ in Diethyl Ether

T,° C	Solute, g	Solvent, g	Concn., m	Association, i
0.067	0.041	32.729	0.051	1.72
0.136	0.098	34.968	0.126	1.89
0.190	0.154	37.197	0.190	2.00
0.311	0.308	43.168	0.326	2.10
0.405	0.486	50.258	0.442	2.19

Table 35. Observed Band Maximas in the Infrared in the Al-H Stretching and Bending Vibrational Regions for Several Alkoxy Derivatives of $LiAlH_4$ in Tetrahydrofuran (Conc.≈0.2 m).

Compound	ν Al-H (cm^{-1})	δ Al-H (cm^{-1})
$LiAlH_4$	1690	765
$LiAl(OCH_3)H_3$	1690	785, 755, 720
$LiAl(OCH_3)_3H$	1690	755
$LiAl(Ot\text{-}Bu)H_3$	1760, 1705	795, 775, 738
$LiAl(Ot\text{-}Bu)_3H$	1760	788, 772
$LiAl(OCHPh_2)H_3$	1690	760
$LiAl(OCHPh_2)_3H$	1800	775, 738

Table 36. Observed Band Maximas in the Infrared in the B-H Stretching Vibrations for Several Alkoxy Derivatives of $LiBH_4$ in Tetrahydrofuran (Conc.≈0.2 m)

Compound	ν B-H (cm^{-1})
$LiBH_4$	2220
$LiB(OCH_3)H_3$	2220
$LiB(OCH_3)_2H_2$	2210
$LiB(OCH_3)_3H$	2210
$LiB(Ot\text{-}Bu)H_3$	2220
$LiB(Ot\text{-}Bu)_3H$	2260
$LiB(OCHPh_2)H_3$	2220
$LiB(OCHPh_2)_3H$	2220

Table 37. Comparison of Center-to-Center Distances Between the Ions in the Ion Pair

Compound	Calculated From Crystalline Radii (A°) [34,35,36]	Calculated From Equation 5 (A°)	Estimated From Dreiding Models(A°)
$LiAlH_4$	3.35	4.9	5.0*
$NaAlH_4$	3.65	4.4	5.5*
$LiBH_4$	3.10	3.3	4.8*
Bu_4NAlH_4	--	5.2	5.0**

*Cation is specifically solvated by four molecules of THF with the anion at the point of closest approach.

**Cation is not specifically solvated by THF with the anion at point of closest approach.

Table 38. Stereoselectivity of Reductions of Ketones with Complex Metal Hydrides in THF.[38] The Numbers Listed are the Percentages of the Less Stable Alcohol Found in the Products (±0.5%).

	$LiAlH_4$	$NaAlH_4$	$LiBH_4$	Bu_4NAlH_4	$LiAl(OCH_3)_3H$[22]	$LiAl(Ot\text{-}Bu)_3H$[22]
4-tert-butyl cyclohexanone	10	13	7	15	-	-
2-methyl-cyclohexanone	24	29	29	26	69	30
3,3,5-trimethyl-cyclohexanone	80	59	53	55	-	95
camphor	91	88	69	88	99	93
norcamphor	91	83	82	74	98	93

LITERATURE CITED*

1. A. E. Fenholt, A. C. Bond and H. I. Schlesinger, Jr., J. Amer. Chem. Soc., 69, 1199 (1947).

2. N. G. Gaylor, "Reductions with Complex Metal Hydrides," Interscience Publications, Inc., New York, N. Y., 1956.

3. M. F. Paddock, Nature, 167, 1070 (1951).

4. G. G. Evans, J. K. Kennedy and F. P. DeGeco, J. Inorg. Nuclear Chem., 4, 40 (1957).

5. G. Jarder and K. Draffezyth, J. Anarg. Chem., 283, 27 (1956).

6. N. M. Alpatova, T. N. Dymava, Y. M. Kessler and O. R. Osepov, Russian Chem. Rev., 37, 99 (1968).

7. H. Noth, Angew. Chem., 73, 371 (1961).

8. N. Skar and B. Post, Inorg. Chem., 6, 669 (1964).

9. S. Abrahams and J. Kalnop, J. Chem. Phys., 22, 434 (1954).

10. K. Nakamota, "Infrared Spectra of Inorganic and Coordination Compounds," John Wiley and Sons, New York, N. Y. (1963).

11. E. Wiberg and H. Graf, Diploma work of H. Graf, University of Munich (1953).

12. E. R. Lippincott, J. Chem. Phys., 17, 1351 (1949).

13. L. D'Or and J. Fuger, Bull. Soc. ray. Sci. Lieye, 25, 14 (1956). C. A. 50:11 114A (1956).

14. H. Haraguchi and S. Fujiwara, J. Chem. Phys., 73, 3467 (1969).

15. R. Dautel and W. Zeil, Z. Electrochem., 64, 1234 (1960).

16. R. Ehrlich, A. Young, G. Rice, J. Dovorak, P. Shapiro and H. F. Smith, J. Amer. Chem. Soc., 88, 858 (1966).

*For complete titles to all journals referred to see Access, 1969.

17. G. Jones and B. Bradshaw, J. Amer. Chem. Soc., 55, 1799 (1933).

18. D. M. Maciner and T. J. Shedlovsky, J. Amer. Chem. Soc., 54, 1429 (1932).

19. T. L. Brown, D. W. Dickerhoof, D. A. Bafus and G. L. Morgan, Rev. Sci. Instr., 33, 491 (1962).

20. D. F. Shriver, "The Manipulation of Air-Sensitive Compounds," McGraw-Hill Book Company; New York, N. Y., 1969.

21. R. Ehrlich, A. Young and Perry, Inorg. Chem., 4, 758 (1965).

22. H. C. Brown and H. R. Deck, J. Amer. Chem. Soc., 87, 5620 (1965).

23. F. W. Walker and E. C. Ashby, J. Chem. Ed., 45, 654 (1968).

24. R. M. Fuoss and F. Accascina, "Electrolytic Conductance," Interscience Publications, Inc., New York, N. Y., 1959.

25. T. E. Hogen-Esch and J. Smid, J. Amer. Chem. Soc., 88, 318 (1966).

26. D. N. Bhattacharyra, C. L. Lee, J. Smid and M. Swarc, J. Phys. Chem., 68, 708 (1965).

27. M. K. Wong, W. J. McKinney and A. Popov, J. Phys. Chem., 75, 56 (1971).

28. C. Lassigne and P. Baine, J. Phys. Chem., 75, 3188 (1971).

29. J. Wuepper and A. Popov, J. Amer. Chem. Soc., 91, 4352 (1969).

30. W. Edgell, J. Lyford, R. Wright, W. Rosen and A. Watts, J. Amer. Chem. Soc., 92, 2240 (1970).

31. R. Dautel and W. Zeil, Z. Elektrochem., 64, 1234 (1960).

32. H. S. Harned and B. B. Owen, "The Physical Chemistry of Electrolytic Solutions," A.C.S. Monograph No. 137, Reinhold, New York, N. Y., 1969.

33. E. Schaschel and M. C. Day, J. Amer. Chem. Soc., 90, 503 (1968).

34. L. Pauling, "Nature of the Chemical Bond," 3rd Ed., Cornell University Press, Ithaca, New York, 1960.

35. P. Ford and R. Richards, Discussions Faraday Soc., 19, 230 (1955).

36. N. Shlav and B. Post, Inorg. Chem., 6, 669 (1967).

37. C. A. Kraus, J. Chem. Ed., 35, 324 (1958).

38. E. C. Ashby and R. Boone, unpublished results.

39. L. G. Savedoff, J. Amer. Chem. Soc., 88, 664 (1966).

VITA

Frank R. Dobbs completed his undergraduate work at the University of Illinois, Chicago, and Roosevelt University, Chicago, Illinois and received his Bachelor of Science Degree in Chemistry in January, 1963. He received a Master of Science Degree in Organic Chemistry under the direction of Professor Harry Cohen at Roosevelt University in August, 1966. He entered the Ph. D. program at Georgia Tech as instructor and began his studies in organometallic chemistry under the direction of E. C. Ashby on September, 1968.

For the last several years, he has been employed in the Chemistry Department as instructor, teaching freshman chemistry at Georgia Tech and Georgia State University. Previously he was employed in various capacities for six years at Witco Chemical Corporation, Chicago, Illinois and attained the position of chief chemist (August, 1966) in charge of pilot plant personnel and coordinated the pilot plant scale synthesis of organic chemicals. He has made contributions in the production of various polyols for rigid and flexible urethane foams, sodium isethionate for bar soaps, and an amine oxide surfactant for hair shampoos. He has recently accepted a position as chemistry specialist with Aerojet Solid Propulsion Company of Sacramento, California.

Frank is a professional chemist, accredited and is a member of the American Institute of Chemists, the American Chemical Society, and the American Association for the Advancement of Science.

He is married to the former Mary Ann Kalata, and they have one daughter, Rita Marie.